KIDNEY WEEK 2025

Renal Biopsy:
Clinical Correlations

Post-Session Syllabus
with answers and discussion

Case 1 from Vanderlene L. Kung, MD, PhD, Oregon Health & Science University

A 40-year-old man with self-reported kidney dysfunction since his 20s, hyperlipidemia, hypertension, and gout presents to re-establish medical care. He has a 20-pack per year cigarette smoking history. No family history is initially obtained. Vitals on admission are all within normal limits. On physical exam, the patient is obese and without any peripheral edema. A comprehensive metabolic panel is notable for elevated serum creatinine of 3.9 mg/dL, hypocalcemia (8.3 mg/dL), and serum albumin within normal limits (3.9 g/dL). No erythrocytes or leukocytes are seen on urinalysis. Urine total protein-to-creatinine ratio is 2.0. Antinuclear antibody (ANA), ANCA, and Hepatitis B (HBV) and C (HCV) serologies are negative. Serum C3 and C4 complement levels are within normal limits. A retroperitoneal ultrasound shows bilateral small kidneys with cortical thinning, increased echogenicity, and bilaterial cortical cysts. A kidney biopsy is performed for CKD with subnephrotic proteinuria.

Biopsy Images

Figure 1. Light microscopy, Jones silver-stained sections:

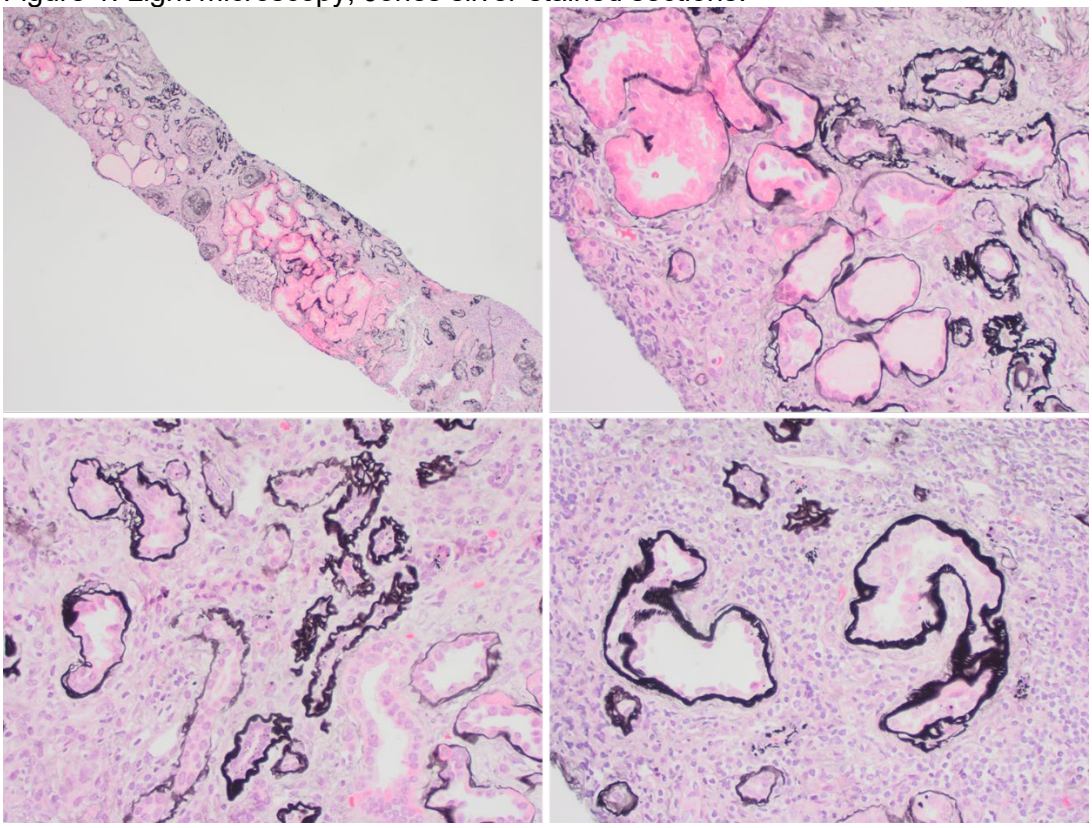

Figure 2. Electron microscopy:

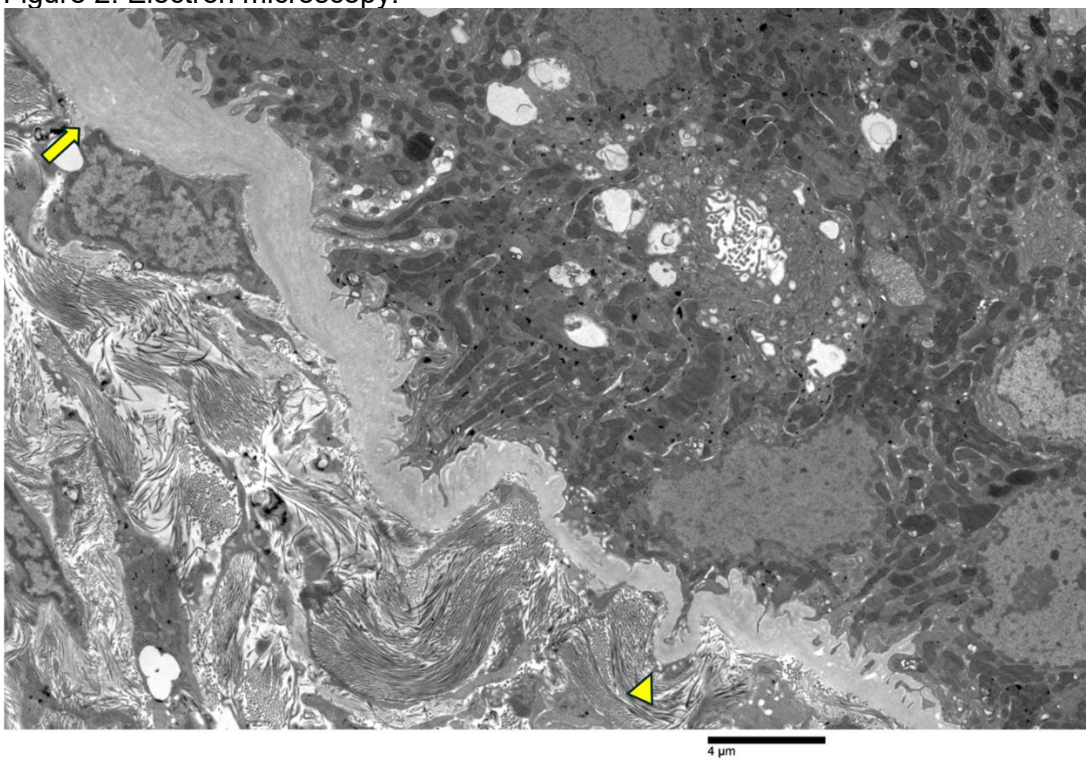

Pathologic Findings

Light Microscopy: The light microscopy tissue consists of portions of renal cortex and corticomedullary junction containing 10 glomeruli, five of which are globally sclerosed. Patent glomeruli are enlarged. Glomerular capillary walls are smooth and single-contoured, and mesangial regions are of normal width and cellularity. There is no endocapillary hypercellularity, segmental sclerosis, or crescentic injury. There is approximately 70% interstitial fibrosis with tubular atrophy, accompanied by dense lymphoplasmacytic interstitial inflammation (Figure 1). Atrophic tubular basement membranes are thickened and double-contoured, and few dilated tubules with irregular basement membranes are seen (Figure 1). Arteries display up to severe intimal fibrosis, and arterioles show severe intimal hyalinosis. There is no vascular inflammation.

Immunofluorescence Microscopy: The immunofluorescence microscopy tissue consists of portions of renal cortex and medulla containing six glomeruli, four of which are globally sclerosed. There is very modest fine granular mesangial staining for IgM and IgA (zero to trace, each). Tubular casts stained for IgA and both kappa and lambda light chains, all at approximately equal intensities. No granular interstitial or tubular basement staining is seen.

Electron Microscopy: The electron microscopy tissue consists of portions of renal cortex containing 10 glomeruli, five of which are globally sclerosed. One glomerulus contains a perihilar segment of sclerosis. Ultrastructural evaluation of two glomeruli shows glomerular capillary basement membranes with corrugation, normal trilaminar structure, and a global increase in thickness. There is partial podocyte foot process effacement. No active electron-dense immune complex-type deposits are identified in any location. No endothelial cell tubuloreticular inclusions are seen. Tubular basement membranes focally show possible variability in thickness, with both segmental thickening (arrow) and segmental thinning (triangle) (Figure 2). No bundled or cystic endoplasmic reticulum is identified in the tubular epithelial cells.

Diagnosis

- Severe interstitial fibrosis with tubular atrophy, chronic interstitial nephritis, and possible tubular basement membrane irregularities
- FSGS, likely secondary
- Severe arterial and arteriolar nephrosclerosis

Clinical Follow-Up

Subsequent correlation with uric acid levels and family history reveals elevated plasma uric acid of 12.6 mg/dL and strong family history of kidney disease. The patient's mother, maternal grandmother, and maternal uncle are all on dialysis, and the patient has one sibling, a brother, who also has CKD.

Genetic testing with a commercially available next-generation sequencing panel identified no *UMOD*, *REN*, *HNF1B*, *SEC61A*, or *DNAJB11* pathogenic variants. *MUC1* genotyping is performed at Wake Forest on the patient's brother to show a pathogenic cytosine insertion within the variable number tandem repeat region of *MUC1* exon 2, diagnostic of autosomal dominant tubulointerstitial kidney disease (ADTKD)-*MUC1*.

The patient is referred for genetic counselling and educated on smoking cessation, continued medical management of hypertension and gout, and eventual need for kidney replacement.

Questions for Case 1

1. The light microscopy in this case shows chronic interstitial nephritis (dense, lymphoplasmacytic inflammation associated with interstitial fibrosis and tubular atrophy, sparing the preserved tubulointerstitium).

All but which scenario can be associated with chronic interstitial nephritis, similar to this case?

A. 5-aminosalicylic acid use
B. History of ifosfamide exposure
C. Vesicoureteral reflux
D. Acute pyelonephritis

Any persistent exposure to a medication that causes allergic acute interstitial nephritis can ultimately result in chronic interstitial nephritis. 5-aminosalicylic acid, frequently used in patients with ulcerative colitis, is notable for inflammation that may persist for months or years after drug discontinuation (A). Similarly, ifosfamide, an alkylating agent used in many chemotherapy regimens, can cause chronic interstitial nephritis along with tubular epithelial cell nuclear atypia that can persist long after drug discontinuation (B). Other than medication-induced inflammation, the chronic interstitial nephritis differential includes reflux/obstruction, autoimmune diseases, and chronic infections (C). Pyelonephritis, if untreated or recurrent, can cause chronic interstitial nephritis; however, acutely, pyelonephritis is characterized by neutrophilic tubulointerstitial inflammation and tubular microabscesses (D).

2. The immunofluorescence microscopy is negative for any tubulointerstitial immune complex deposits in this case.

   What tubulointerstitial diseases are associated with tubular basement membrane immune deposits? Select all that apply.

   A. IgG4-related kidney disease
   B. Antibrush border antibody disease
   C. ADTKD-*UMOD*
   D. Sjogren syndrome

   ADTKD is not an immune complex-mediated disease, and no immune deposits are seen in any of the ADTKD subtypes (C). Granular tubular basement staining for IgG and both kappa and lambda light chains is typical in IgG4-related kidney disease (A) and antibrush border antibody disease (B), and can also be seen in Sjogren syndrome (D).

3. **What ultrastructural alterations in tubular basement membranes can be seen in ADTKD?**

   A. Duplication, lamellation, irregular thickness, and disruption
   B. Collagen bundles
   C. Electron-dense immune complex-type deposits
   D. Amorphous powdery deposits

   Segmental tubular basement membrane duplication, lamellation, irregular thickness, and/or disruption can be seen in ADTKD (A). However, these ultrastructural features are not sensitive or specific for ADTKD. Tubular basement membrane thickening is a feature of tubular atrophy, and uniform thickening in the absence of atrophy can be seen in diabetic nephropathy. Tubular basement membrane collagen bundles can be seen in LMX1B-associated nephropathy (B). Tubular basement membrane immune complex deposits can be seen in autoimmune tubulointerstitial nephritides and in lupus nephritis (C). Amorphous powdery deposits along tubular basement membranes are seen in monoclonal immunoglobulin deposition disease (D).

Discussion

ADTKD is the third most common genetic cause of kidney disease worldwide after ADPKD and Alport syndrome.[1] ADTKD used to be grouped with medullary cystic kidney disease and nephronophthisis, but it is now understood to be distinct from these ciliopathies. Additional previous terms used to describe what is now known as ADTKD include familial juvenile hyperuricemic nephropathy and uromodulin-associated kidney disease. Now, per KDIGO guidelines, ADTKD is subtyped by the affected gene.[2] Currently, seven affected genes have been identified, defining ADTKD-*UMOD*, ADTKD-*MUC1*, ADTKD-*REN*, ADTKD-*HNF1B*, ADTKD-*SEC61A*, ADTKD-*DNAJB11*, and ADTKD-*APOA4*. Reflecting the possibility of additional yet-to-be-characterized affected genes and barriers to genetic testing, there is an additional diagnostic category of ADTKD-not otherwise specified (NOS). ADTKD diagnosis requires family history compatible with autosomal dominant inheritance, with compatible kidney histopathology and/or demonstration of a pathogenic variant in one of the ADTKD genes in an affected individual or at least one family member.[2]

ADTKD-*MUC1* is the second most common ADTKD subtype after ADTKD-*UMOD* and makes up approximately 20% of ADTKD cases.[3,4] *MUC1* encodes a glycoprotein, mucin 1, expressed

by thick ascending limb and distal convoluted tubular epithelial cells, as well as epithelial cells throughout the body, and has roles in barrier defense and cell signaling. *MUC1* pathogenic variants result in an abnormal accumulation of mucin 1 in tubular epithelial cells. Most *MUC1* pathogenic variants cannot be detected by current commercially available sequencing panels. More than 90% of cases of ADTKD-*MUC1* are due to nonsense mutations from a cytosine insertion in the variable number tandem repeat (VNTR) region of *MUC1* exon 2, resulting in a truncated mucin 1 protein.[5,6] Commercially offered exome sequencing panels rely on sequencing of short reads and are thus unable to detect variants in regions with highly recurrent motifs or repeats, as is the case within the *MUC1* VNTR region.[7] As a result, *MUC1* pathogenic variants can only be detected by polymerase chain reaction (PCR) amplification of the *MUC1* VNTR region followed by long-read sequencing[8] or special computational pipelines designed to detect cytosine insertion in the *MUC1* VNTR from short-read sequencing data.[6,9]

ADTKD-*MUC1* is clinically characterized by decline in kidney function, usually starting in adolescence and generally progressing to ESKD by middle-age. Penetrance is complete, but disease severity and age of onset is variable. A positive family history is typical, as is a bland urinalysis with minimal to no proteinuria and no hypertension, at least early in the disease course. Ultrasound shows normal to small kidneys, with cysts usually seen when disease is advanced. Patients are frequently hyperuricemic and have gout. Median kidney survival is 46 years.[3] There are no therapies to delay CKD progression in ADTKD, and thus treatment is limited to supportive measures, including management of hyperuricemia/gout and sequela of CKD. Genetic counseling is recommended at diagnosis, and genetic testing should be performed on prospective living related kidney donors. ADTKD does not recur following transplantation, and for all ADTKD subtypes, age-adjusted transplant outcomes are comparable to those of kidney transplant recipients with other etiologies of ESKD.[10,11]

The kidney biopsy findings of ADTKD are nonspecific. Particularly in the absence of known family history of kidney diseases, ADTKD can be easily overlooked as a diagnostic consideration. In one study of predominantly US ADTKD patients, ADTKD was only suspected on kidney biopsy in 6% of cases.[12] Similarly, in a cohort of Japanese ADTKD patients, there was clinical suspicion for ADTKD in only 58% of individuals with genetically confirmed ADTKD, and ADTKD was not invoked as a diagnostic consideration within the biopsy report of nearly 60% of patients with ADTKD later confirmed by genetic testing.[4] Biopsies show increased interstitial fibrosis/tubular atrophy, involved by lymphoplasmacytic interstitial inflammation. Tubular basement membrane irregularities (segmental thickening, thinning, and multilayering) are best seen on periodic acid-Schiff (PAS) and silver stains by light microscopy and can also be appreciated by electron microscopy. Advanced cases show microcystic dilation of tubules, though this is not a specific finding. Glomeruli are unaffected, but increased global glomerulosclerosis and secondary FSGS occur in advanced disease. Immunofluorescence is negative for any glomerular or tubulointerstitial complement or immunoglobulin deposition. Ultrastructural evaluation can show tubular basement membrane irregular thickening, splitting, and duplication. Truncated mucin 1 protein can be immunodetected in ADTKD-*MUC1*; however, staining for this protein is not routinely available in clinical labs. In patients where other causes of chronic interstitial nephritis can be excluded (e.g., medication exposure, chronic infection, autoimmune disease, and metabolic disorders), findings of chronic interstitial nephritis with tubular cysts, tubular basement irregularities, and negative immunofluorescence should prompt correlation with uric acid levels and family history.

References

1. Groopman, E.E., et al., Diagnostic Utility of Exome Sequencing for Kidney Disease. *N Engl J Med*, 2019. 380(2): p. 142-151.
2. Eckardt, K.U., et al., Autosomal dominant tubulointerstitial kidney disease: diagnosis, classification, and management--A KDIGO consensus report. *Kidney Int*, 2015. 88(4): p. 676-83.
3. Olinger, E., et al., Clinical and genetic spectra of autosomal dominant tubulointerstitial kidney disease due to mutations in UMOD and MUC1. *Kidney Int*, 2020. 98(3): p. 717-731.
4. Tanaka, Y., et al., Phenotype and genotype of autosomal dominant tubulointerstitial kidney disease in a Japanese cohort. *Clin Exp Nephrol*, 2025. 29(6): p. 788-796.
5. Yamamoto, S., et al., Analysis of an ADTKD family with a novel frameshift mutation in MUC1 reveals characteristic features of mutant MUC1 protein. *Nephrol Dial Transplant*, 2017. 32(12): p. 2010-2017.
6. Bensouna, I., et al., Systematic Screening of Autosomal Dominant Tubulointerstitial Kidney Disease- MUC1 27dupC Pathogenic Variant through Exome Sequencing. *J Am Soc Nephrol*, 2025. 36(2): p. 256-263.
7. Kirby, A., et al., Mutations causing medullary cystic kidney disease type 1 lie in a large VNTR in MUC1 missed by massively parallel sequencing. *Nat Genet*, 2013. 45(3): p. 299-303.
8. Okada, E., et al., Detecting MUC1 Variants in Patients Clinicopathologically Diagnosed With Having Autosomal Dominant Tubulointerstitial Kidney Disease. *Kidney Int Rep*, 2022. 7(4): p. 857-866.
9. Saei, H., et al., VNtyper enables accurate alignment-free genotyping of MUC1 coding VNTR using short-read sequencing data in autosomal dominant tubulointerstitial kidney disease. *iScience*, 2023. 26(7): p. 107171.
10. Stavrou, C., et al., Outcome of kidney transplantation in autosomal dominant medullary cystic kidney disease type 1. *Nephrol Dial Transplant*, 2003. 18(10): p. 2165-9.
11. Cormican, S., et al., Renal transplant outcomes in patients with autosomal dominant tubulointerstitial kidney disease. *Clin Transplant*, 2020. 34(2): p. e13783.
12. Bleyer, A.J., et al., Variable clinical presentation of an MUC1 mutation causing medullary cystic kidney disease type 1. *Clin J Am Soc Nephrol*, 2014. 9(3): p. 527-35.

Case 2 from Mercury Y. Lin, MD, Cedars-Sinai Medical Center

A 60-year-old woman presents to urgent care with a history of hypertension and a baseline serum creatinine level of 0.8 mg/dL. She was reportedly in her usual state of health until five days ago, at which time she began experiencing fatigue, nausea, chills, and sore throat. She became febrile (temperature of 103° F at home) and has had episodes of vomiting. She denies abdominal pain and dysuria. The patient did not receive COVID-19 vaccination but denies loss of taste or smell. Her vital signs are temperature of 104° F, BP of 103/70, BMI 28, pulse of 104/min, respiratory rate of 20, and oxygen saturation of 96%. Her outpatient medication consists of metoprolol 50 mg twice daily.

On physical exam, she is well-developed, well-nourished, and alert and awake. There is no skin rash and no palpable lymphadenopathy. There is no report of hepatosplenomegaly. Lung and heart sounds are unremarkable. There is no lower extremity edema.

A portable chest radiograph is obtained and shows normal cardiomediastinal silhouette and no infiltrate. Clinical laboratory evaluation reveals serum creatinine of 3.7 mg/dL (eGFR 15 mL/min/173 m^2), blood urea nitrogen of 38 mg/dL, glucose of 171 mg/dL, and albumin of 2.9 g/dL. Aspartate aminotransferase and alanine aminotransferase are within normal limits. Her complete blood count is within normal limits (white blood cells 8.2 K/uL, hemoglobin 11.8 g/dL, hematocrit 35.6%, and platelets 365 K/uL). Urinalysis reveals 1+ proteinuria, 3–10 red blood cells (RBCs) per high power field, negative urine nitrite, and negative urine leukocyte esterase. COVID-19 and rapid Streptococcus A tests are negative. She is diagnosed with acute kidney failure and is admitted to a community hospital. Additional inpatient laboratory studies reveal positive ANA, negative ANCA, negative cryoglobulin test, low serum complement levels, and a kappa:lambda light chain ratio of 1.5 (ref range: 0.26 to 1.65). She is started on empiric antibiotic therapy. Nephrology consultation is obtained, and a kidney biopsy is performed.

Biopsy Images

Light Microscopy:

Jones silver stain:

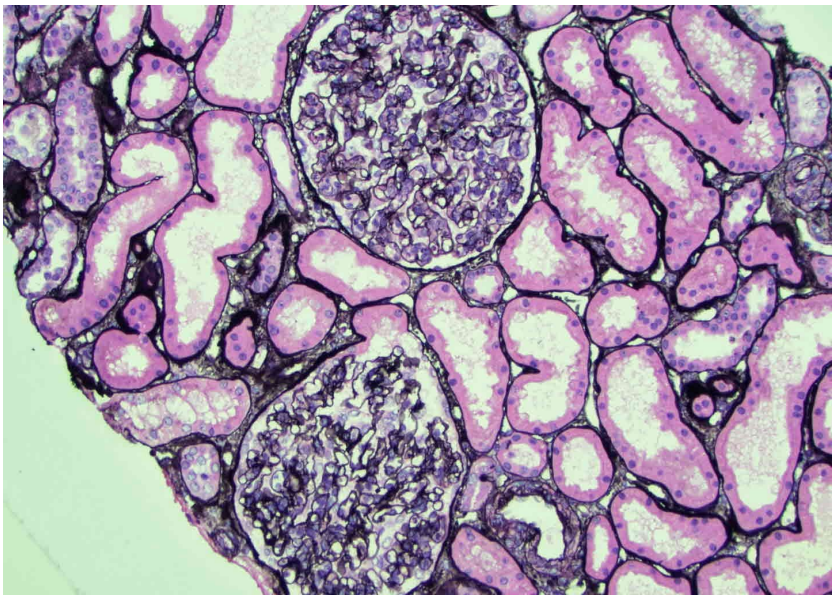

Jones silver stain:

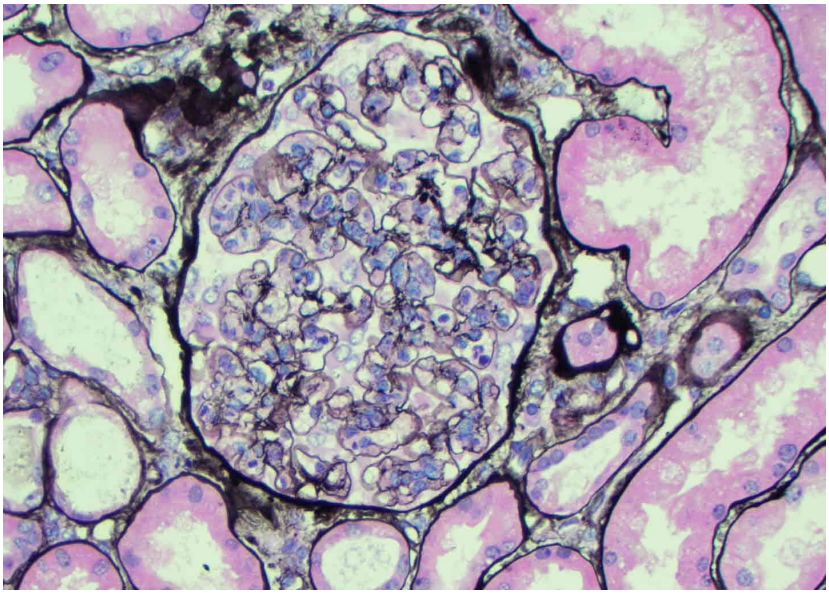

PAS stain:

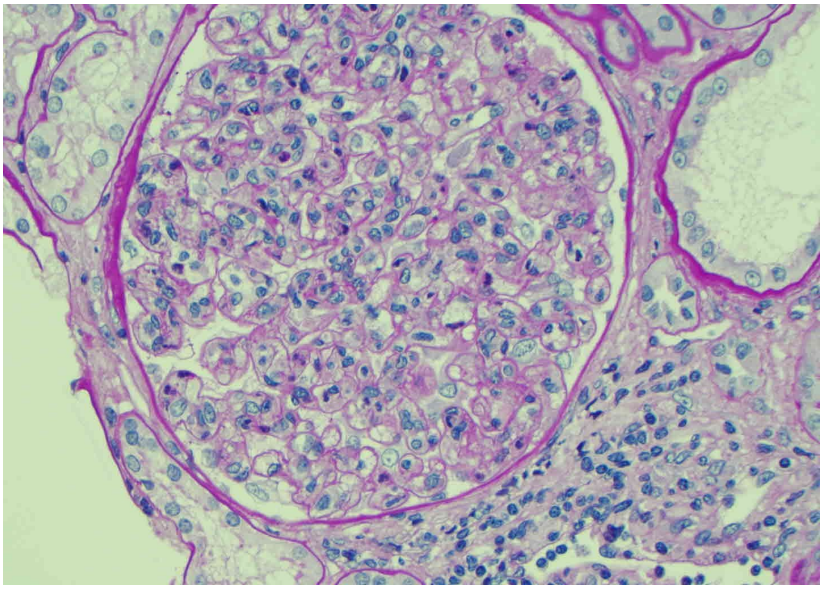

Masson trichrome:

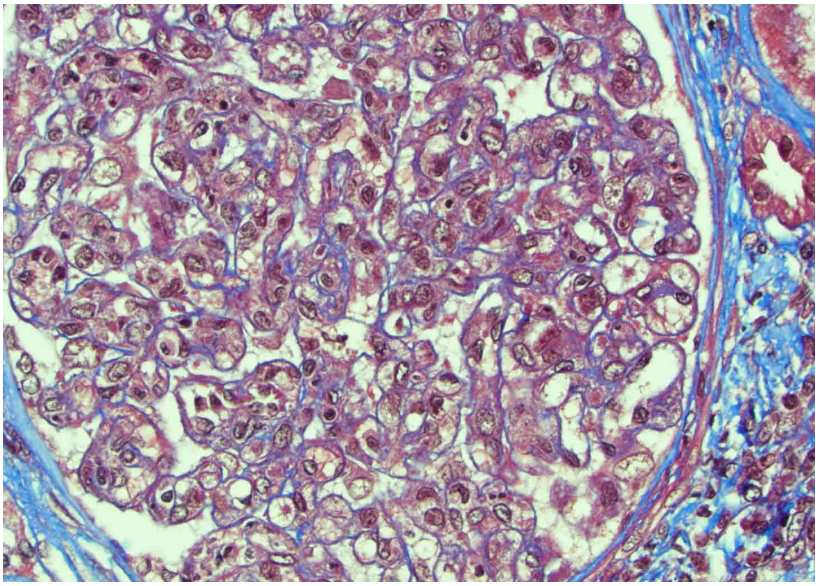

CD68:

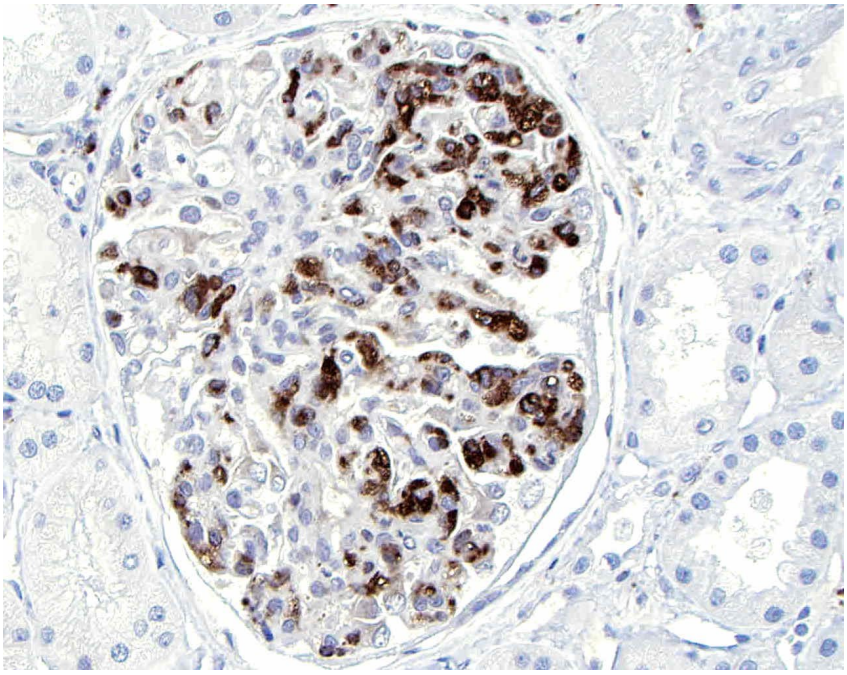

Masson trichrome:

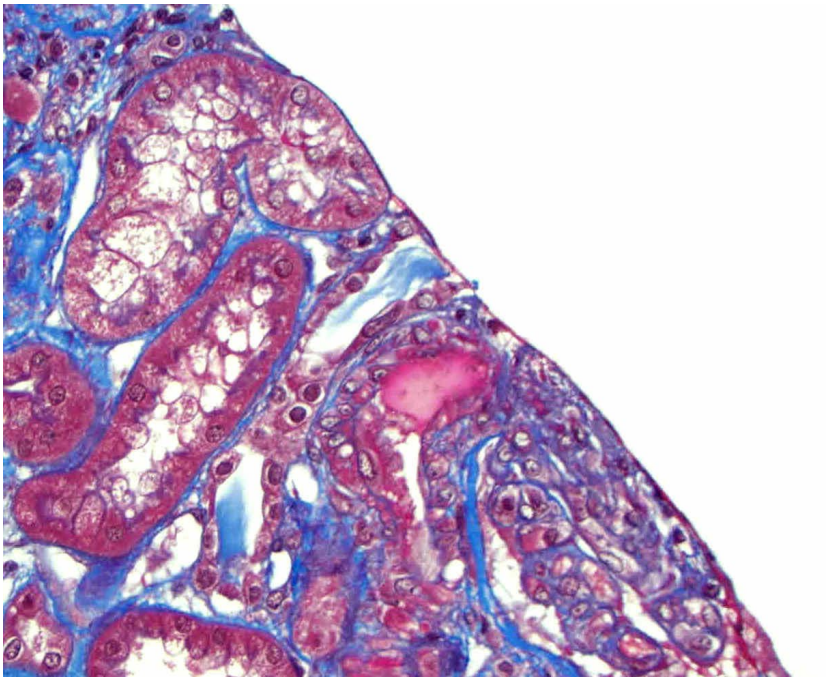

Immunofluorescence Microscopy: Noncontributory.

Electron Microscopy:

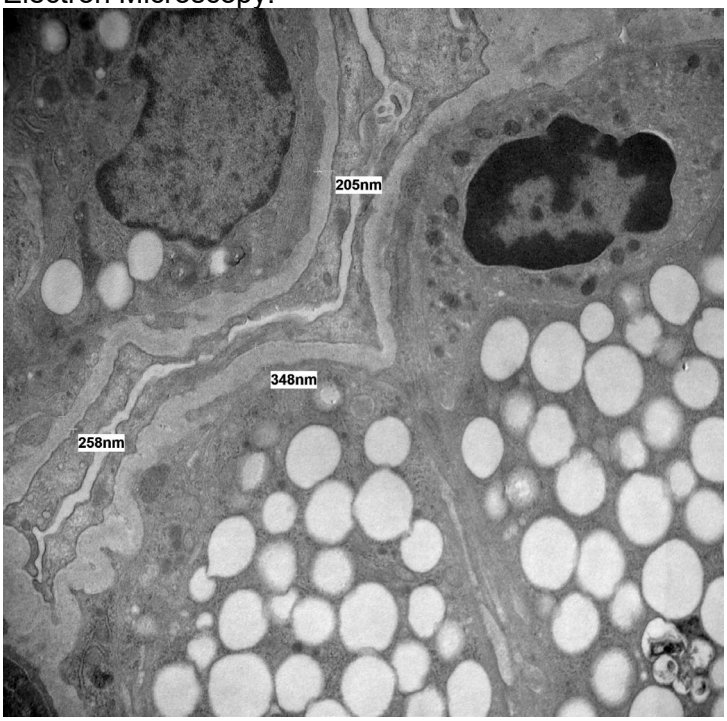

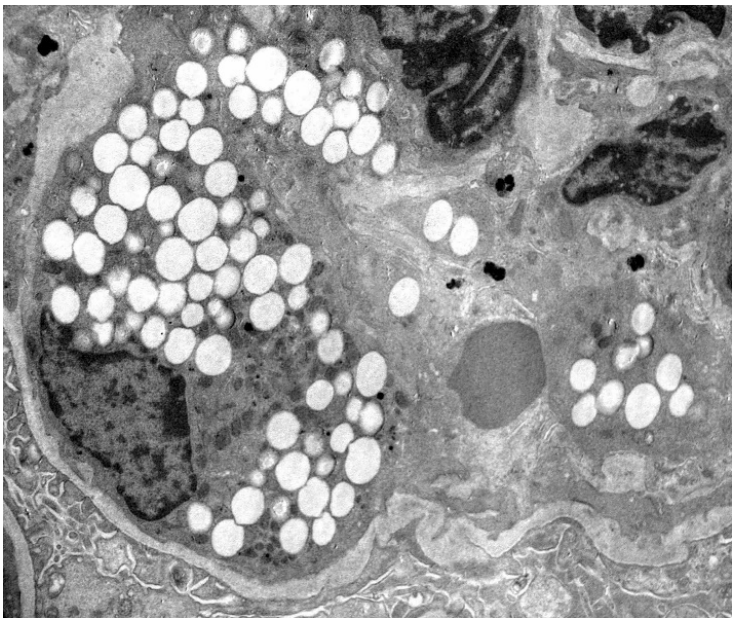

Pathologic Findings

Light Microscopy: There are two cores of renal cortex and medulla. There are 20 glomeruli, of which three are globally sclerosed. There is no segmental glomerulosclerosis or fibrous crescent. In remaining nonsclerotic glomeruli, few appear mildly enlarged. Glomerular capillary walls display rare double contours and are without subepithelial "spikes" or craters. There is endocapillary hypercellularity, characterized mostly prominently by intracapillary histiocytes/ macrophages (highlighted by CD68 IHC). There are fewer intracapillary CD3+ lymphocytes and granulocytes. "Cryo plugs" are not identified. There are focal mesangiolyses. There is no cellular crescent. Tubular segments are acutely injured with attenuation of epithelial lining, diminished brushed borders, and intraluminal shedding of cells. There is patch interstitial edema. There is minimal interstitial inflammation. A mild degree of tubulointerstitial scarring is noted. Arteries show severe intimal fibrosis. Very rarely, a hilar arteriole with intraluminal fibrin thrombus is detected. There is no vasculitis.

Immunofluorescence Microscopy: There are four glomeruli, of which two are globally sclerosed. In nonsclerotic glomeruli, there is no immune reactant staining in glomerular capillaries, glomerular mesangial areas, or podocytes. Tubular casts show normal immune reactant staining for IgA and kappa and lambda light chains.

Electron Microscopy: Ultrastructural examination of four nonsclerotic glomeruli reveals capillary basement membranes with normal architectural organization, which are either normal in thickness or segmentally thin. There are no lacunae/vacuoles within glomerular capillary walls. There is estimated 80% podocyte foot process effacement. There are many intracapillary foamy histiocytes/macrophages. Rarely, there are probable phagocytized RBCs within histiocytes. There are no intracytoplasmic crystalline inclusions. There is segmental subendothelial widening, and some glomerular endothelial cells are swollen with loss of fenestrations. Endothelial tubuloreticular inclusions are not identified. Fibrin tactoids and lamellated lipid material are not identified within glomerular capillary lumina. Immune complex-type electron dense deposits are not identified in glomerular and extraglomerular compartments.

Diagnosis

- Histiocytic glomerulopathy
- A rare, thrombosed arteriole
- Acute tubular injury
- Severe arterial nephrosclerosis

Clinical Follow-Up

The patient's serum creatinine peaks at 5.6 mg/dL during hospital admission. After establishing a tissue diagnosis of histiocytic glomerulopathy, IV methylprednisolone is promptly initiated. Afterwards, her clinical symptoms subside, and she is no longer febrile. After nine days of hospitalization, her serum creatinine normalizes to 0.87 mg/Dl, and she is discharged home on a steroid taper. She has outpatient follow-up with nephrology, rheumatology, and hematology. Her serum complement levels also normalize, and her kappa:lambda light chain ratio remains within normal limits (1.2–1.5). However, a faint IgG-lambda paraprotein is later detected during hematology workup.

Approximately one year after initial hospitalization, she is readmitted to the hospital with acute kidney failure with a serum creatinine level of 3.7 mg/dL. A repeat kidney biopsy during this admission reveals persistent/recurrent histiocytic glomerulopathy. However, it is a limited biopsy, and it is not possible to evaluate for renal parenchymal scarring. Another course of IV methylprednisolone is started, and her serum creatinine normalizes after a few weeks.

Three years after her initial hospitalization and diagnosis of histiocytic glomerulopathy, aside from the single episode of relapse, the patient has been doing well. Presently, her medications include oral prednisone 5 mg and mycophenolate 2000 mg daily. Her most recent serum creatinine level is 0.73 mg/dL, and she has no proteinuria.

Questions for Case 2

1. **To highlight intracapillary histiocytes in histiocytic glomerulopathy, what is the most appropriate immunohistochemical stain?**

    A. CD1a
    B. CD3
    C. CD20
    D. CD31
    E. CD68

    CD68 is a lysosomal marker used to identify histiocytic and monocytic cells (E). CD3 is a maker for T lymphocytes (B), and CD20 is a marker for B lymphocytes (C). CD31 is a marker for endothelial cells (D). CD1a is a normal T lymphocyte surface antigen, and in the context of histiocytic proliferation, it is used as marker for Langerhans cell histiocytosis (A).

2. A 75-year-old man presents with multiple myeloma and glomerulopathy characterized by many intracapillary CD68+ histiocytes showing bright lambda light chain staining, no kappa light chain staining, and numerous crystalline deposits detected by electron microscopy.

   What is the most accurate diagnosis?

   A. Histiocytic glomerulopathy
   B. Crystal-storing histiocytosis, lambda light chain
   C. Glomerular thrombotic microangiopathy (TMA)
   D. Cryoglobulinemic glomerulonephritis
   E. Lipoprotein glomerulopathy

   In this patient with plasma cell neoplasm and glomerular histiocytes laden with lambda light chain crystals, the diagnosis would be a crystal-storing histiocytosis (B). Histiocytic glomerulopathy (A), glomerular TMA, and lipoprotein glomerulopathy would be devoid of biased immunoglobulin light chain staining and light chain crystals. Intracapillary immune aggregates ("cryo plugs") are present in cryoglobulinemic glomerulonephritis (D). For glomerular TMA, endothelial cell injury and fibrin tactoids are the prominent features (C). Lipoprotein glomerulopathy is characterized by pale staining lipoprotein thrombi in glomerular capillary lumina (E).

3. **Under electron microscopy, which ultrastructural finding is commonly observed in histiocytic glomerulopathy?**

   A. Mesangial immune complex deposits
   B. Mesangial lipid debris
   C. Endothelial tubuloreticular inclusions
   D. Focal glomerular endothelial swelling and loss of fenestrations
   E. Lamellated podocyte lipid inclusions

   Features of low-grade TMA (e.g., focal endothelial swelling, loss of fenestrations, subendothelial widening, and mesangiolysis) are common in histiocytic glomerulopathy (D). Mesangial immune complex deposits are typical of diseases such as IgAN (A). Mesangial lipid debris is seen in patients with chronic liver disease and has been termed "hepatic glomerulosclerosis" (B). Endothelial tubuloreticular inclusions are nonspecific and usually described in patients with autoimmune diseases (e.g., systemic lupus erythematosus) or viral infections (e.g., HCV, HBV, HIV, and SARS-CoV-2) (C). Lamellated podocyte lipid inclusions can be seen with drug exposure (such as hydroxychloroquine, amiodarone, and gentamicin), Fabry disease, or other lysosomal storage diseases (E).

Discussion

Histiocytic glomerulopathy is a glomerular lesion characterized by extensive glomerular infiltration by CD68+ histiocytes; it is associated with hemophagocytic syndrome/ hemophagocytic lymphohistiocytosis/macrophage activation syndrome (HPS/HLH/MAS).[1–4] HPS, HLH, and MAS are synonymous terms used in the medical literature. While MAS was initially coined to describe HPS occurring in the setting of autoimmune/autoinflammatory diseases, it no longer retains such specificity and is seemingly a more appropriate terminology in situations when hemophagocytosis (macrophages with ingested hematopoietic elements) cannot be histologically documented.[4] HPS/HLH/MAS describes a severe and potentially fatal inflammatory syndrome characterized by activation of cytotoxic lymphocytes, proliferation of

macrophages through interferon-gamma pathway, and subsequent cytokine production (including tumor necrosis factor-alpha and interleukin-1 and -6) resulting in a cytokine storm.[3–5] HPS/HLH/MAS can occur as a "primary"/familial disease due to mutations in genes involved with function of cytotoxic lymphocytes and natural killer cells, or as a "secondary" phenomenon due to infection, malignancy, autoimmune/autoinflammatory disease, metabolic disease, or organ transplantation.[5–7] Usual clinical features include fever, splenomegaly, cytopenias, hypertriglyceridemia, hypofibrinogenemia, hemophagocytosis (usually detected by biopsy of bone marrow, spleen, or lymph node), elevated ferritin, and elevated serum-soluble CD25. Per the 2024 Histocyte Society diagnostic criteria, at least five of the aforementioned eight features need to be present for a clinical diagnosis of HPS/HLH/MAS.[1,4,5] While clinical involvement of the kidneys with AKI is also common, it is not presently considered in the diagnostic criteria.

More recently, a "renal-limited" form of HPS/HLH/MAS has been described in patients with AKI and histiocytic glomerulopathy but less severe systemic manifestation. It has been postulated that this renal-limited form of the disease could be attributed to disproportionate activation of macrophage phenotypes in the kidney environment (i.e., prophagocytic tissue-resident macrophages vs. proinflammatory/cytokine-producing bone marrow-derived macrophages).[3] This case appears to reflect a "renal-limited" HPS/HLH/MAS.

From a histopathologic diagnostic prospective, histiocytic glomerulopathy displays a striking appearance. However, there are other entities with glomerular capillary histiocyte/macrophage infiltration by light microscopy that can mimic histiocytic glomerulopathy. These mimics include crystal-storing histiocytosis, cryoglobulinemic glomerulonephritis, glomerular TMA, lecithin-cholesterol acyltransferase deficiency, and lipoprotein glomerulopathy.[2] With the exception of glomerular TMA, the remaining entities in the histopathologic differential diagnosis can generally be distinguished when interpreted with immunofluorescence and electron microscopy findings, clinical history, and other laboratory studies. Differentiating between histiocytic glomerulopathy and glomerular TMA can be uniquely challenging since low-grade features of TMA are commonly present in histiocytic glomerulopathy.[1–3] Further complicating this diagnostic dilemma is a recent study reporting under recognition of TMA in HPS/HLH/MAS.[8] Given the overwhelming morphologic evidence of histiocytic glomerulopathy in this case, the rare detected thrombosed arteriole was regarded as a separate vascular lesion and not contrary to the principal diagnosis of histiocytic glomerulopathy. Although not a part of this histopathologic differential diagnosis, it should be recognized that podocytopathies (e.g., minimal change disease (MCD) and collapsing glomerulopathy) have also been reported in patients with HPS/HLH/MAS.[3]

Treatment decisions for HPS/HLH/MAS require consideration of the severity of hyperinflammation, the suspected trigger, and chronic medical conditions. Although there is no randomized control trial, immunomodulatory therapy with glucocorticoids, anti-IL-1 drugs, and/or intravenous immunoglobulin have demonstrated improvement in most patients irrespective of underlying etiology.[3,5] In the presented case, the patient is on low-dose oral prednisone and mycophenolate and has preserved kidney function three years after initial diagnosis.

References

1. Santoriello, Dominick, et al. Hemophagocytic Syndrome with Histiocytic Glomerulopathy and Intraglomerular Hemophagocytosis. *American Journal of Kidney Diseases*, vol. 67, no. 6, 8 Jan. 2016, pp. 978–983.
2. Kaur, Amulyajit, and Sanjeev Sethi. Histiocytic and Nonhistiocytic Glomerular Lesions: Foam Cells and Their Mimickers. *American Journal of Kidney Diseases*, vol. 67, no. 2, 19 Nov. 2015, pp. 329–336.
3. Uchida, Takahiro, and Takashi Oda. Concept and Diagnostic Challenges of Renal-Limited Hemophagocytic Syndrome/Macrophage Activation Syndrome. *Journal of Clinical Medicine*, vol. 13, no. 8, 9 Apr. 2024, pp. 2161–2161.
4. Pouneh Dokouhaki, et al. Histiocytic Glomerulopathy Associated with Hemophagocytic Lymphohistiocytosis. *Kidney Medicine*, vol. 4, no. 2, 8 Dec. 2021, pp. 100396–100396,
5. Edward, Filippone, and Farber John. Hemophagocytic lymphohistiocytosis: An Update for Nephrologists. *Int Urol Nephrol*, vol. 48, 20 Apr. 2016, pp. 1291–1304.
6. Kentaro Sugisaki, et al. Glomerular Lipidosis as a Feature of Renal-Limited Macrophage Activation Syndrome in a Transplanted Kidney: A Case Report. *BMC Nephrology*, vol. 24, no. 1, 7 Nov. 2023.
7. Hiser, Wesley, et al. Hemophagocytic Syndrome with Histiocytic Glomerulopathy Associated with Ovarian Serous Carcinoma. *Baylor University Medical Center Proceedings*, vol. 34, no. 1, 19 Aug. 2020, pp. 153–155.
8. Minoia, Francesca, et al. Thrombotic Microangiopathy Associated with Macrophage Activation Syndrome: A Multinational Study of 23 Patients. The Journal of Pediatrics, vol. 235, 1 Aug. 2021, pp. 196–202.

Case 3 from Cathryn J. Lapedis, MD, MPH, MSc, University of Michigan

A 68-year-old white man with a history of smoking (unknown amount, quit 35 years ago), hypertension, stroke, type 2 diabetes, gout, and arthritis presents to nephrology due to increasing creatinine up to 2.8 mg/dL (up from 2.2 mg/dL 5 months prior). Per a clinical note, a potential diagnosis of lupus nephritis is under consideration due to a positive dsDNA of 39 IU/mL in January 2025, and ANA has been negative. Prior rheumatology evaluation in 2016 showed ANA-negative, normal complements, and a confirmed diagnosis of arthritis and gout with no evidence of lupus. Additional labs provided at the time of biopsy include: Creatinine of 2.83 mg/dL (eGFR 23), glucose high at 168 mg/dL, ANA-negative. Urinalysis shows: Negative leukocyte esterase; negative for white and red blood cells; no squamous epithelial cells, no bacteria, and no hyaline casts; albumin-to-creatinine ratio of 2141 mg/g creatinine; and HbA1c 6.7%. Recent testing for complements, lactate dehydrogenase, and haptoglobin were not completed. Medications include spironolactone, vitamin C, zinc, turmeric root extract, dulaglutide, multivitamin, amlodipine/benazepril, duloxetine, doxazosin, coenzyme Q10, colchicine, vitamin D3, carvedilol, aspirin, canagliflozin, hydralazine, and chlorthalidone. The patient has a history of fentanyl use for severe pain but has been weaned off opioids after a long withdrawal period. This biopsy is to determine the etiology of his proteinuria and CKD.

Biopsy Images

Stained sections of representative glomeruli:

Figure 1: Light microscopy, Jones silver stain 4x, cortex:

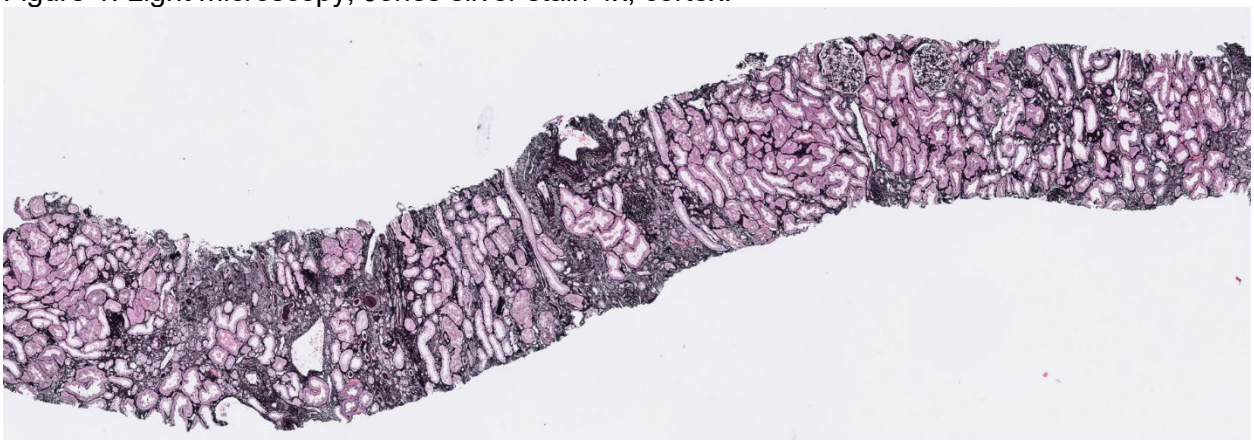

Figure 2: Light microscopy, PAS 20x:

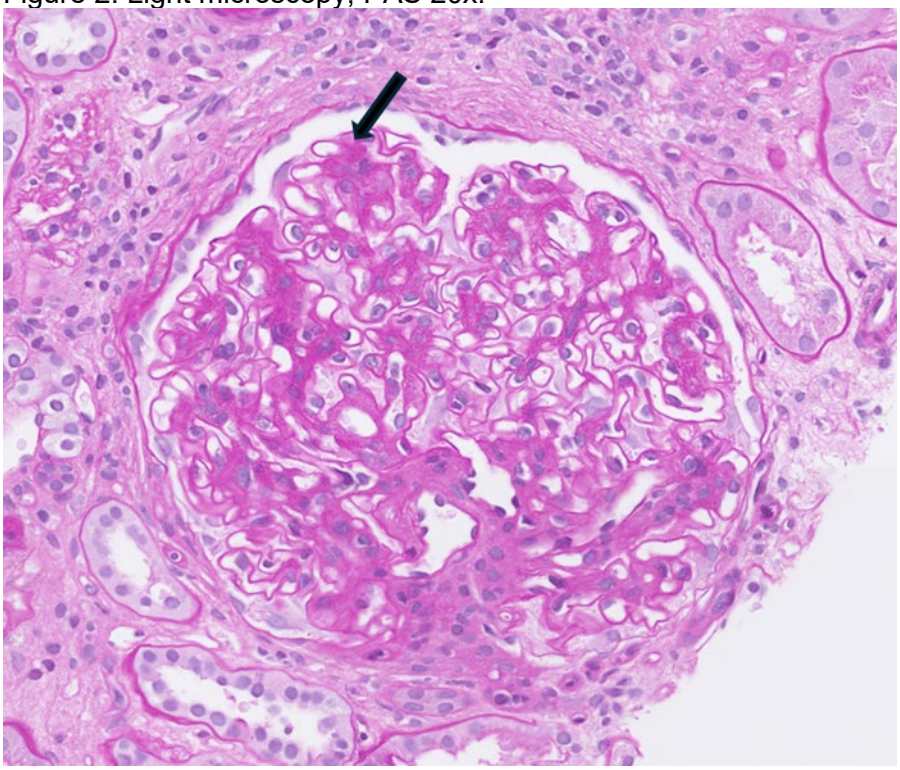

Figure 3: Light microscopy, PAS stain 20x:

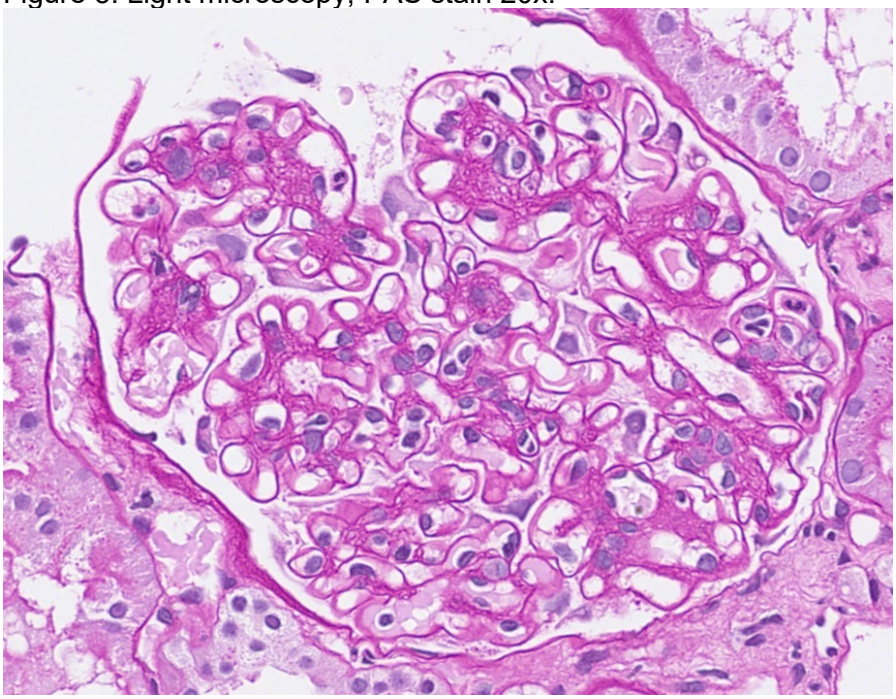

Figure 4: Light microscopy, Jones silver stain, 30x (same glomerulus as Figure 3):

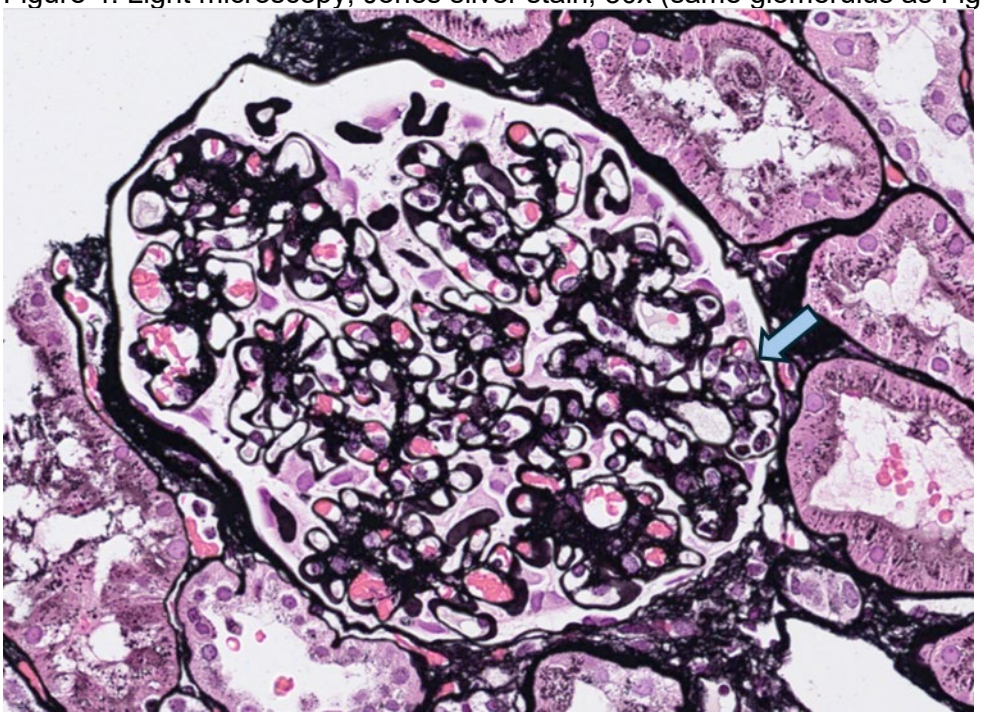

Figure 5: Light microscopy, Jones silver stain, 30x:

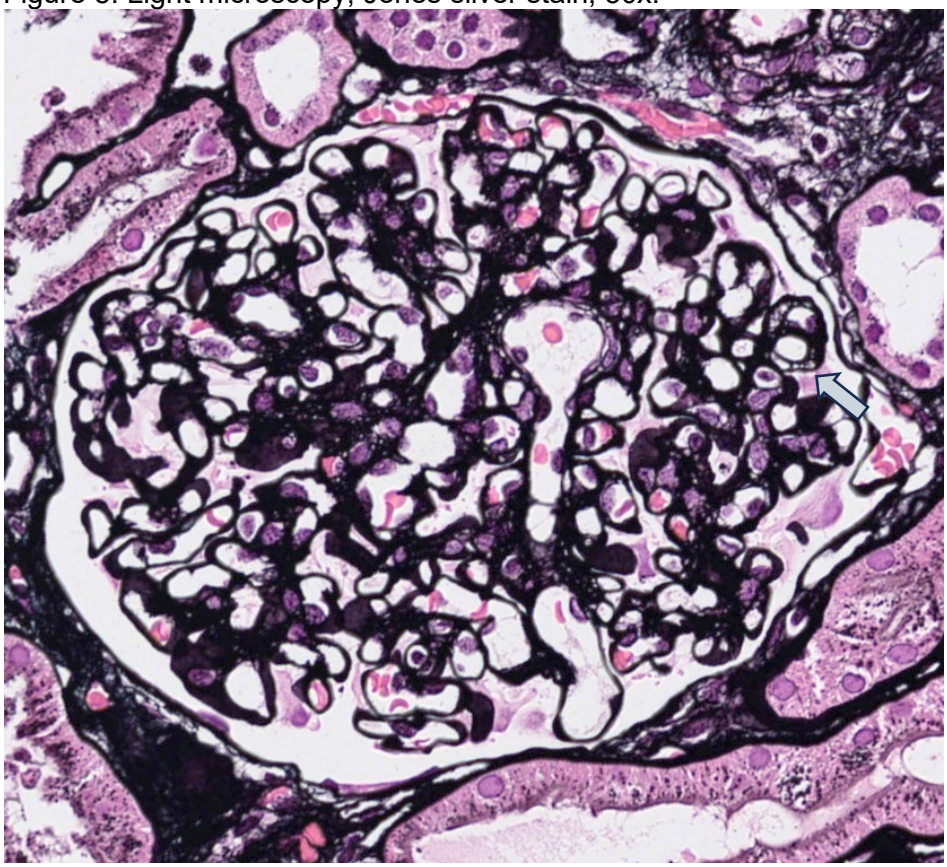

Figure 6. Immunofluorescence, IgA:

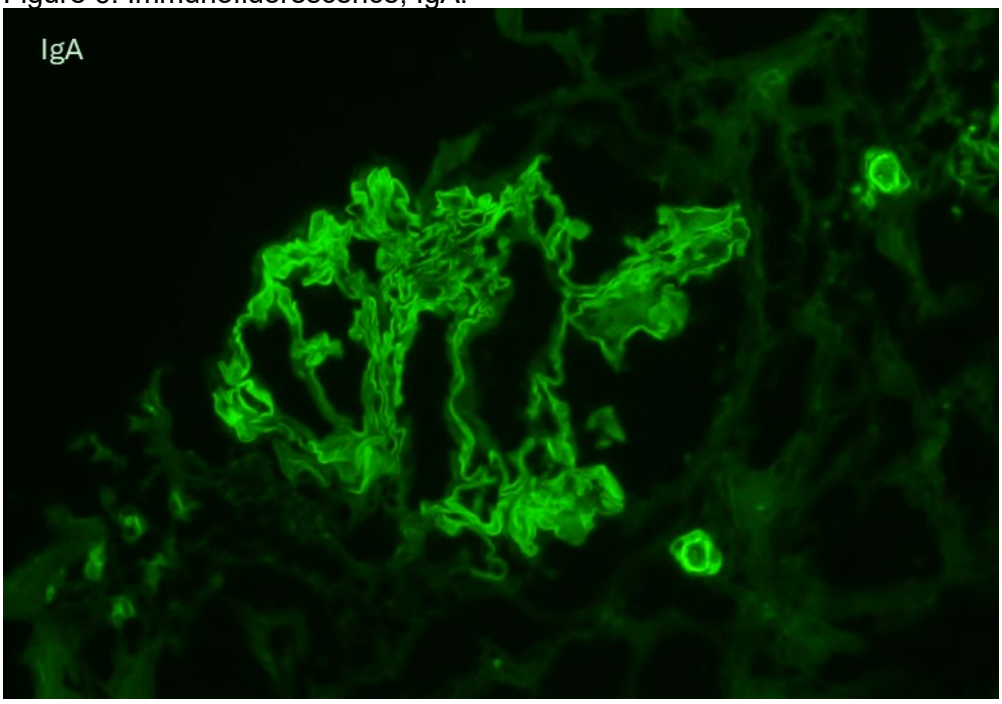

Figure 7. Immunofluorescence, lambda:

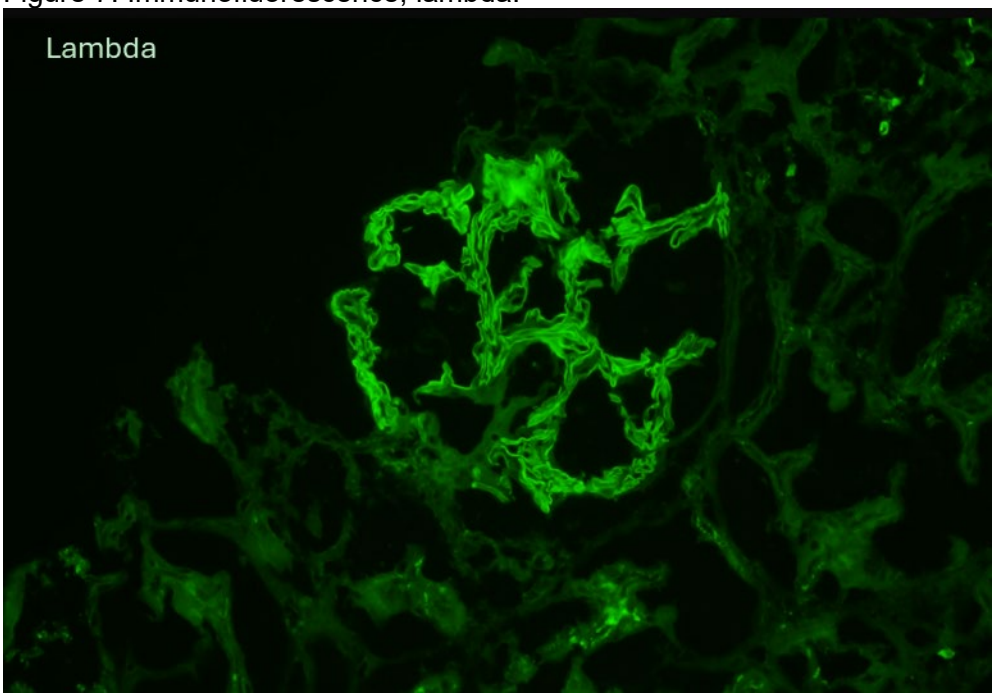

Figure 8. Immunofluorescence, kappa:

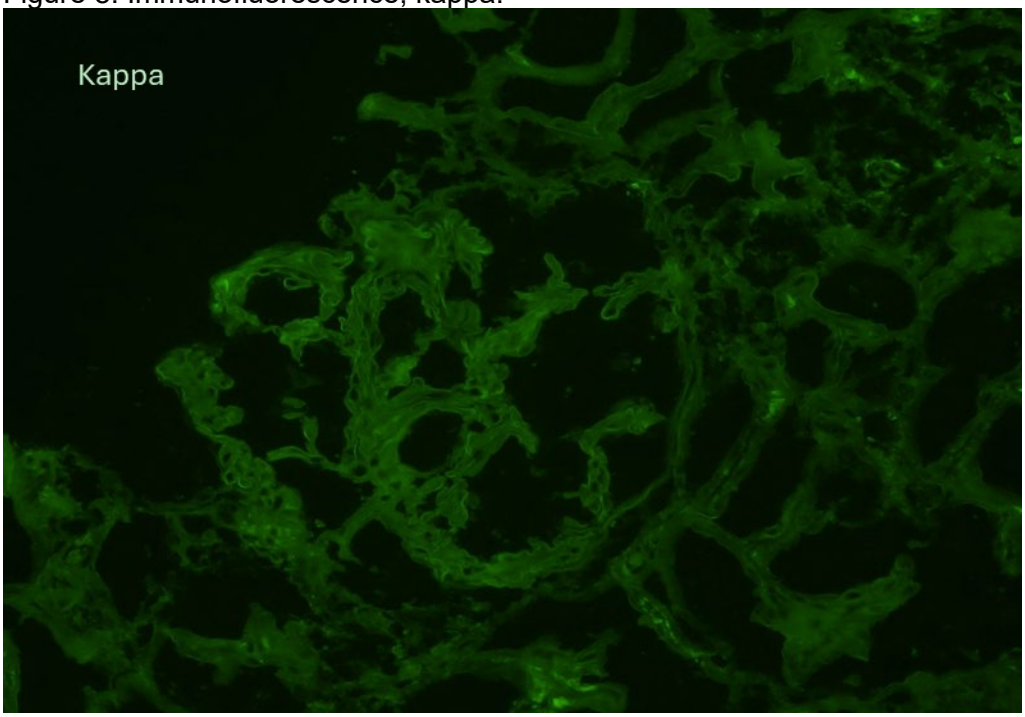

Figure 9. Electron microscopy:

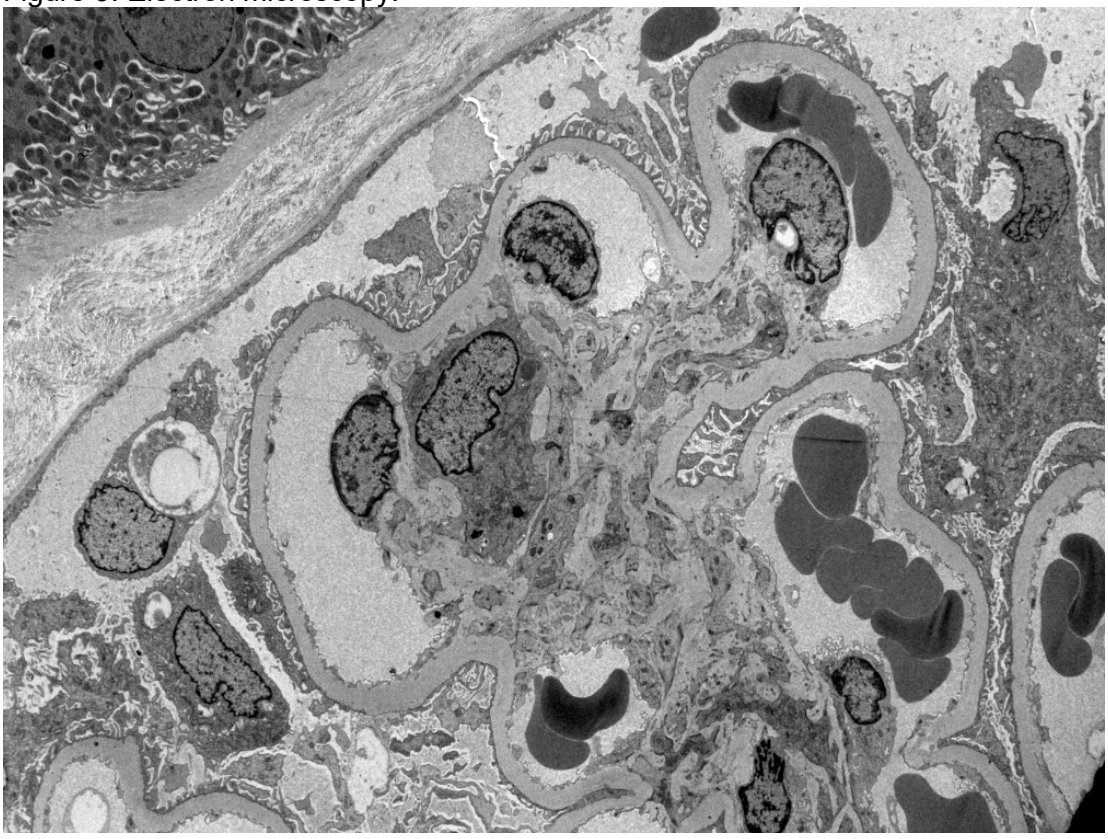

Figure 10. Electron microscopy:

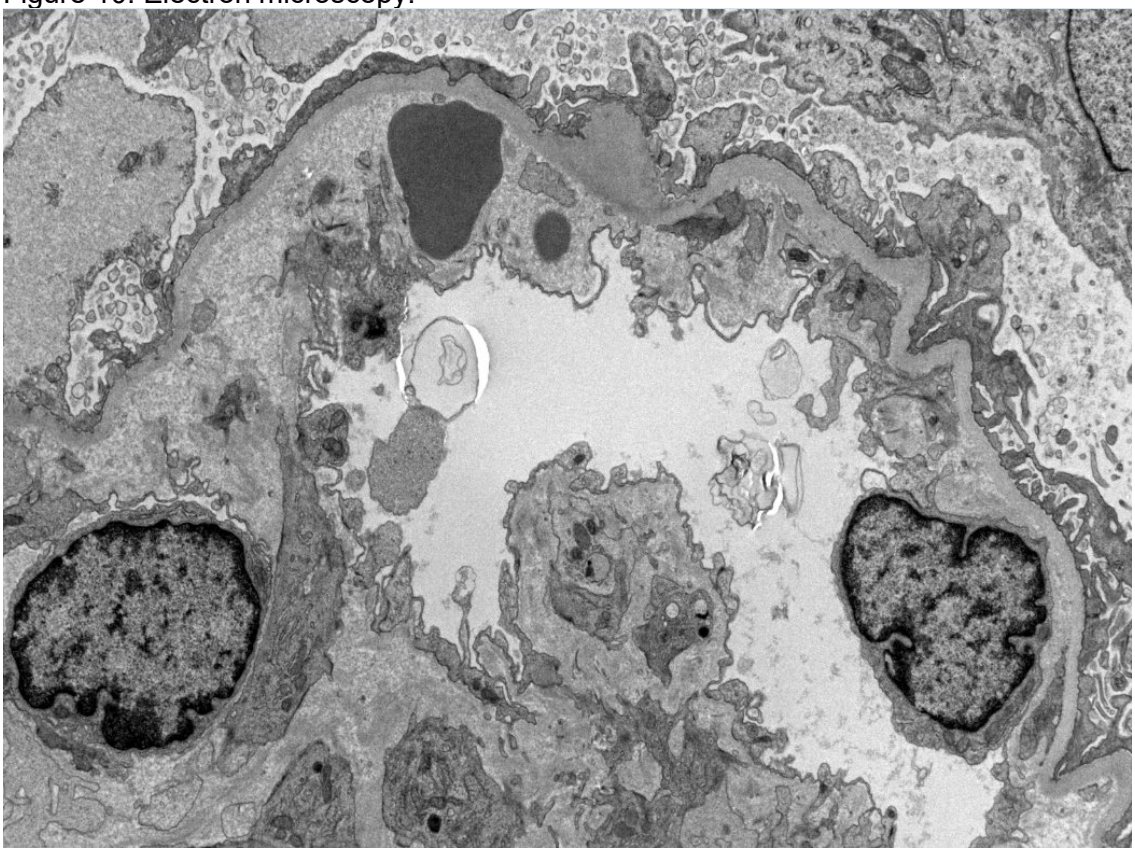

Figure 11. Electron microscopy:

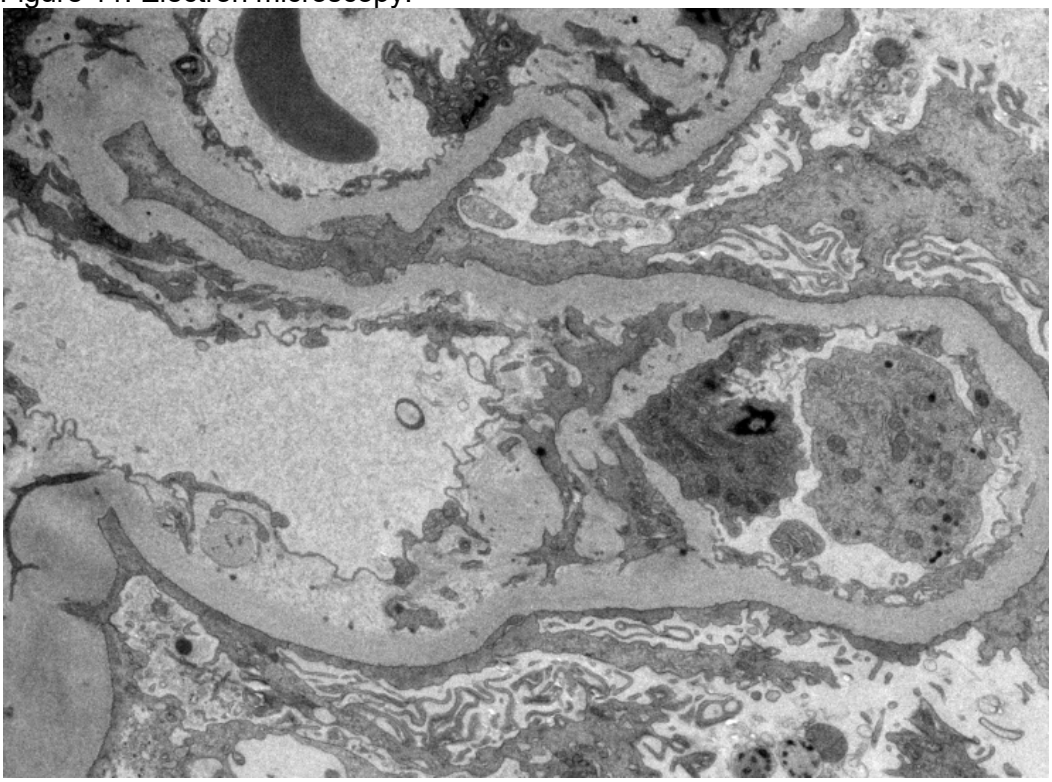

Pathologic Findings

Light Microscopy: The sample consists of renal cortex with 12 glomeruli, of which four are globally sclerosed. The glomeruli are enlarged. The mesangium is mildly to moderately expanded by extracellular matrix and increased numbers of mesangial cells. There are no definitive Kimmelstiel-Wilson nodules. The GBMs appear mildly thickened. There are rare double contours in the GBMs. There are no definitive spikes or craters. One or two glomeruli show endocapillary hypercellularity. There are no crescents. Nonatrophic tubules are enlarged and show mild distension. There is focal loss of the brush border of the proximal tubular epithelium. Few tubules contain PAS-positive hyaline casts. The interstitium contains moderate interstitial inflammation, primarily in areas of atrophy. The infiltrates are composed of mononuclear and scattered plasma cells with rare eosinophils. Approximately 30% of the renal cortex shows interstitial fibrosis and tubular atrophy. Arteries and arterioles show moderate focal sclerosis. One arteriole shows probable focal hyaline degeneration (best seen on silver stain).

Immunofluorescence Microscopy: The sample contains six glomeruli. There are three globally sclerosed glomeruli. There is diffuse linear reactivity for IgA (2+) and lambda (2+); kappa and IgG are negative. Nonspecific irregular segmental reactivity for IgM (trace), C3 (3+), and C1q (2+) are noted in sclerosed glomeruli. Tubules contain few intraluminal casts reactive for polyclonal IgA. The interstitium reveals scattered fibrin deposits. There is no difference in reactivity between kappa and lambda light chains in the tubular casts and background of the tissue.

Electron Microscopy: The sample submitted for electron microscopy examination contains four glomeruli, two of which are globally sclerosed. Two glomeruli are examined ultrastructurally. The glomerular visceral epithelial cells reveal mild to moderate segmental effacement of their foot processes. In rare capillary loops, the subendothelial space of the basement membrane is segmentally expanded by electron-lucent fluffy material and rare fragmented RBCs, and a new layer of basement membrane material is formed under the displaced endothelium (double contour). Rare endothelial cells show focal swelling and a loss of fenestrations. The GBMs are mildly thickened. The mesangium reveals mild expansion of the mesangial matrix, with some irregular densities and the deposition of cellular debris. There are no tubuloreticular inclusions. There are no definitive electron-dense deposits in the capillary loops or mesangium.

Diagnosis and Interpretation

- Glomerulopathy with linear deposition of IgA/lambda on immunofluorescence microscopy, consistent with the so-called monotypic variant of atypical anti-GBM disease
- Diabetic nephropathy, with mild to moderate focal mesangial sclerosis, Renal Pathology Society Class IIa

Questions for Case 3

1. **In Figures 3 and 4 (PAS and Jones silver stain), what glomerular pattern of injury is depicted?**

    A. Crescentic glomerulonephritis
    B. Endocapillary hypercellularity
    C. Normal glomerulus
    D. Membranous glomerulonephritis

    There is an increase in inflammatory cells in the glomerular capillary loops in Figures 3 and 4, indicating the presence of endocapillary hypercellularity (B). There is no evidence of cells within the Bowman space, fibrin, or necrosis, ruling out a crescentic pattern of injury (A). The presence of endocapillary hypercellularity means that this is not a normal glomerulus (C). Finally, a membranous pattern of injury would show thickened GBMs with spikes and craters on the Jones silver stain (D).

2. **How do you interpret the immunofluorescence microscopy findings (Figures 6, 7, and 8) from the biopsy?**

    A. Nonspecific linear staining, nondiagnostic
    B. Linear capillary wall staining for IgA and lambda
    C. Mesangial staining for IgA and lambda
    D. Granular capillary wall staining for IgA and lambda

    The immunofluorescence studies show global linear capillary wall staining for IgA and lambda (B), and kappa is negative. While not exceptionally strong, the pattern of staining is linear and clearly in the capillary walls of the glomeruli in IgA and lambda, while clearly negative in kappa, ruling out nonspecific staining (A). The staining is not in the mesangium (C), and it is smooth and linear without any punctate granularity (D).

3. **What is the pattern of injury seen in the electron microscopy image in Figure 10?**

    A. Mesangiolysis
    B. Subendothelial deposits
    C. Double contour
    D. Normal capillary loop

    The electron microscopy image shows a capillary loop with subendothelial expansion by electron-lucent material, and an entrapped fragmented RBC. A second layer of GBM material overlies the area of subendothelial expansion (double contour) (C). It shows a somewhat expanded mesangium but no evidence of mesangiolysis (A), the subendothelial material is electron-lucent, not -dense (B), and the presence of subendothelial widening, entrapped RBC fragments, and a double contour is not normal for a capillary loop (D).

Follow-Up

Based on the presence of linear IgA/lambda staining, additional laboratory testing is performed. This shows: Urine protein-to-creatinine ratio of 1641 mg/g creatinine, anti-GBM antibody-negative, serum kappa light chains 309 mg/L (normal 3.3–19.4 mg/L), serum lambda light chains 123 mg/L (normal 5.71–26.3 mg/L), serum kappa/lambda ratio elevated at 2.51 (normal 0.26–1.65). Monoclonal gammopathy with IgG/kappa specificity (0.1 gm/dL) is detected on serum immunofixation. Bone marrow biopsy and urine plasmapheresis are pending.

Discussion

This biopsy shows linear glomerular capillary loop staining for IgA and lambda with negative kappa and IgG on immunofluorescence microscopy. There are no electron-dense deposits on electron microscopy. These features, in combination with focal segmental endocapillary hypercellularity and ultrastructural evidence of endothelial cell injury and focal double contours, are consistent with the so-called atypical anti-GBM disease, monotypic variant (IgA/lambda). The pattern of injury includes endocapillary hypercellularity and focal thrombotic microangiopathy (GBM duplication).

This is an incredibly rare diagnosis with only 45 cases reported in the literature.[1–5] Most cases show linear IgG staining, and a very small number show IgA linear staining.[1–5] About half of the reported cases of atypical anti-GBM nephritis show monotypic deposits, staining for one immunoglobulin heavy chain class and one light chain.[1,4] The International Kidney and Monoclonal Gammopathy Research Group includes the monotypic variant of atypical anti-GBM nephritis in the "miscellaneous" subcategory of monoclonal gammopathy of renal significance-associated lesions.[4,6] This monotypic variant of atypical anti-GBM nephritis is less likely to show glomerular crescents, and generally, in these patients, there is no associated detectable circulating monoclonal protein or monoclonal gammopathy to correspond with the monoclonal protein seen on the biopsy.[4] Interestingly, the monotypic variant has been shown to recur in transplants in a small series of patients, suggesting the role of a circulating factor targeting basement membrane collagens that has yet to be identified.[4,7] In this patient, the ratio of kappa-to-lambda free light chains are elevated with a tiny IgG/kappa monoclonal (0.1 gm/dL), which does not correspond with the IgA/lambda immunofluorescence staining.

Atypical anti-GBM nephritis typically presents as a slowly progressive glomerulonephritis with some hematuria, heavy proteinuria, and no lung involvement. In these cases, the serum anti-GBM antibody is negative, and the patterns of injury can be varied, including endocapillary hypercellularity, mesangial hypercellularity, membranoproliferative, focal crescentic glomerulonephritis, glomerular microangiopathy, and FSGS.[4] As noted above, typically 50% are monotypic. Rare cases (12%) in the French cohort show linear IgA.[3]

Generally, this disease is significantly less aggressive than typical anti-GBM disease and has a more slowly progressive renal insufficiency, hematuria, and proteinuria.[3] Summaries of treatments and outcomes are present in the references below. Some patients are treated with immunosuppressive therapies. The literature notes that "monotypic cases would benefit from sensitive techniques, such as serum immunoblot and bone marrow molecular studies, to reveal a possible B-cell disorder and support the hypothesis of a monoclonal gammopathy-induced renal injury."[3]

Additionally, in this biopsy, there are features of diabetic nephropathy, including mesangial sclerosis and thickened GBMs. Mesangial sclerosis can also be seen in cases of atypical anti-GBM disease, so it is unclear exactly what is due to diabetes and what is related to the monotypic variant of atypical anti-GBM disease.

References

1. Nasr SH, Collins AB, Alexander MP, Schraith DF, Herrera Hernandez L, Fidler ME, Sethi S, Leung N, Fervenza FC, Cornell LD. The clinicopathologic characteristics and outcome of atypical anti-glomerular basement membrane nephritis. *Kidney Int*. 2016 Apr;89(4):897-908.
2. Mignano SE, Nasr SH, Fidler ME, Herrera Hernandez LP, Alexander MP, Sethi S, Messias N, Alhamad T, Alrata L, Albadri ST, Cornell LD. Recurrent atypical antiglomerular basement membrane nephritis in the kidney transplant. *Am J Transplant*. 2024 Jan;24(1):123-133.
3. Chauveau B, Gibier JB, Olagne J, Morel A, Aydin S, McAdoo SP, Viallet N, Perrochia H, Pambrun E, Royal V, Demoulin N, Kemeny JL, Philipponnet C, Hertig A, Boffa JJ, Plaisier E, Domenger C, Brochériou I, Deltombe C, Duong Van Huyen JP, Buob D, Roufosse C, Hellmark T, Audard V, Mihout F, Nasr SH, Renaudin K, Moktefi A, Rabant M; CFPR–French Nephropathology Group. Atypical Anti-Glomerular Basement Membrane Nephritis: A Case Series From the French Nephropathology Group. *Am J Kidney Dis*. 2024 Jun;83(6):713-728.e1.
4. Cornell LD. Anti-Glomerular Basement Membrane Disease: Broadening the Spectrum. *Am J Kidney Dis*. 2024 Jun;83(6):701-703.
5. Bharati J, Yang Y, Sharma P, Jhaveri KD. Atypical Anti-Glomerular Basement Membrane Disease. *Kidney Int Rep*. 2023 Mar 21;8(6):1151-1161.
6. Leung N, Bridoux F, Batuman V, Chaidos A, Cockwell P, D'Agati VD, Dispenzieri A, Fervenza FC, Fermand JP, Gibbs S, Gillmore JD, Herrera GA, Jaccard A, Jevremovic D, Kastritis E, Kukreti V, Kyle RA, Lachmann HJ, Larsen CP, Ludwig H, Markowitz GS, Merlini G, Mollee P, Picken MM, Rajkumar VS, Royal V, Sanders PW, Sethi S, Venner CP, Voorhees PM, Wechalekar AD, Weiss BM, Nasr SH. The evaluation of monoclonal gammopathy of renal significance: a consensus report of the International Kidney and Monoclonal Gammopathy Research Group. *Nat Rev Nephrol*. 2019 Jan;15(1):45-59.
7. Mignano SE, Nasr SH, Fidler ME, Herrera Hernandez LP, Alexander MP, Sethi S, Messias N, Alhamad T, Alrata L, Albadri ST, Cornell LD. Recurrent atypical antiglomerular basement membrane nephritis in the kidney transplant. *Am J Transplant*. 2024 Jan;24(1):123-133.

Case 4 from Sujal Shah, MD, Brigham and Women's Hospital

A 41-year-old man with schizophrenia on paliperidone and a history of smoking, stopped years ago, is admitted to the hospital with several weeks of fluid retention/generalized anasarca and weight gain (up to 230 pounds from baseline around 160 pounds). He first noticed this as swelling in his legs, corresponding to a new exercise regimen; the swelling then extended into his testicles and then his abdomen. More recently, he has noticed difficulty breathing. He does not report any changes in urine habits or appetite. The only new medication he is on is a diuretic, which was started for the swelling but has not been effective in decreasing it. There is no remarkable family history.

On admission, he has a BP reading of 143/95, but his vitals are otherwise unremarkable. On physical exam, the abdomen is distended with fluid, and the extremities reveal edema. A comprehensive metabolic panel is notable for elevated serum creatinine of 2.70 mg/dL (reported baseline ~1mg/dL), hypocalcemia (8.0 mg/dL), and markedly low serum albumin (1.4 g/dL). Urinalysis reveals 4+ protein, and a 24-hour urine study reveals proteinuria of 22.34g. Serologies are not ordered by the clinical team, as the feeling is that they would not preclude the need for biopsy.

The patient is started on furosemide and has a "great response". He is not initially started on steroids due to mental health history and the good response to furosemide. He is discharged home with a plan for outpatient kidney biopsy, which is performed three weeks later.

Biopsy Images

Figure 1. Light microscopy, Jones silver stain 4x, cortex:

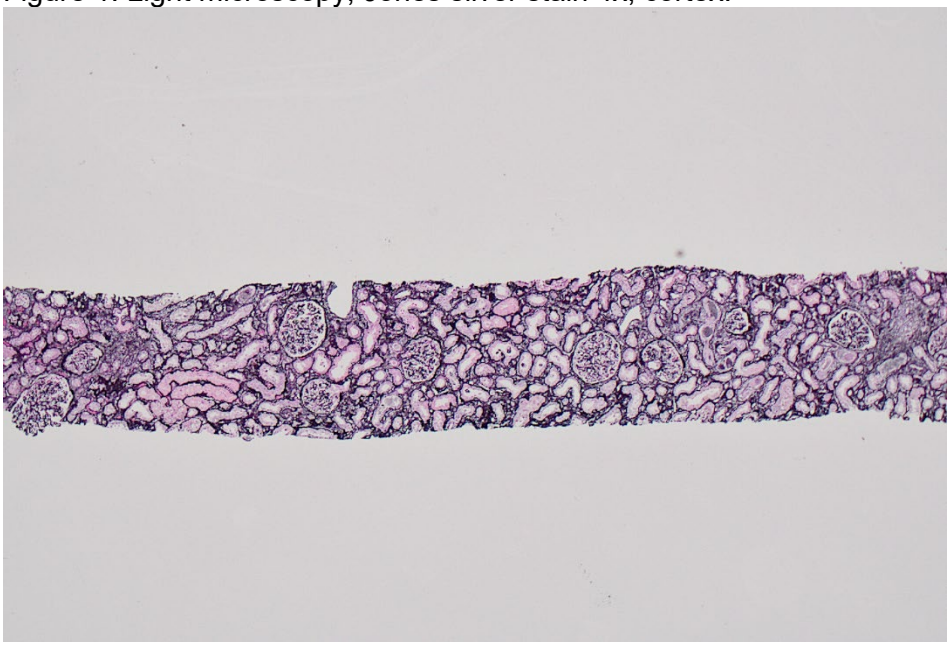

Figure 2. Light microscopy, PAS 10x, cortex:

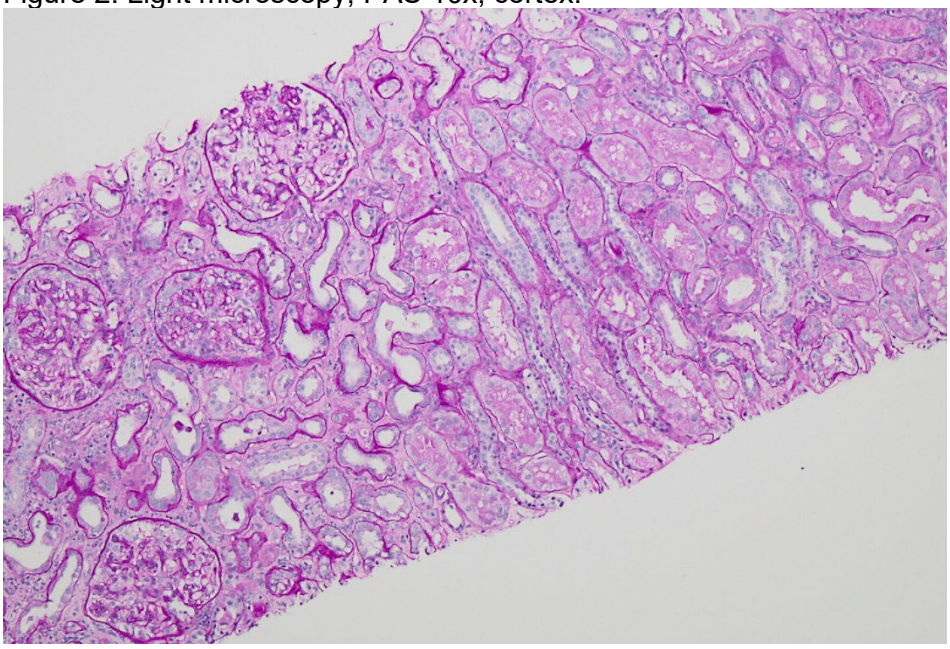

Figure 3. Light microscopy, hematoxylin and eosin (H&E) 40x, representative glomeruli:

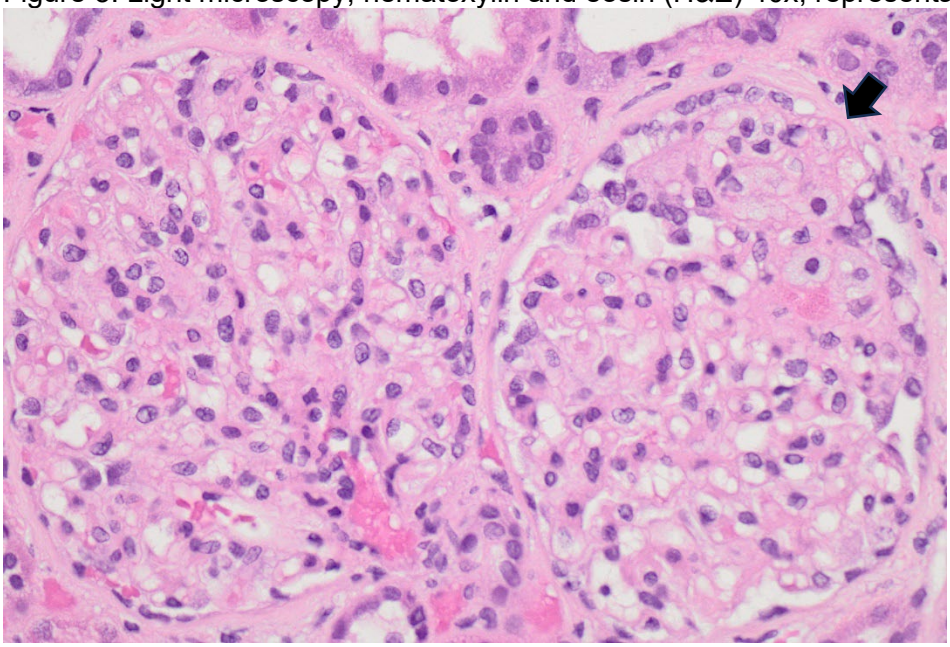

Figure 4. Light microscopy, PAS 40x, representative glomeruli:

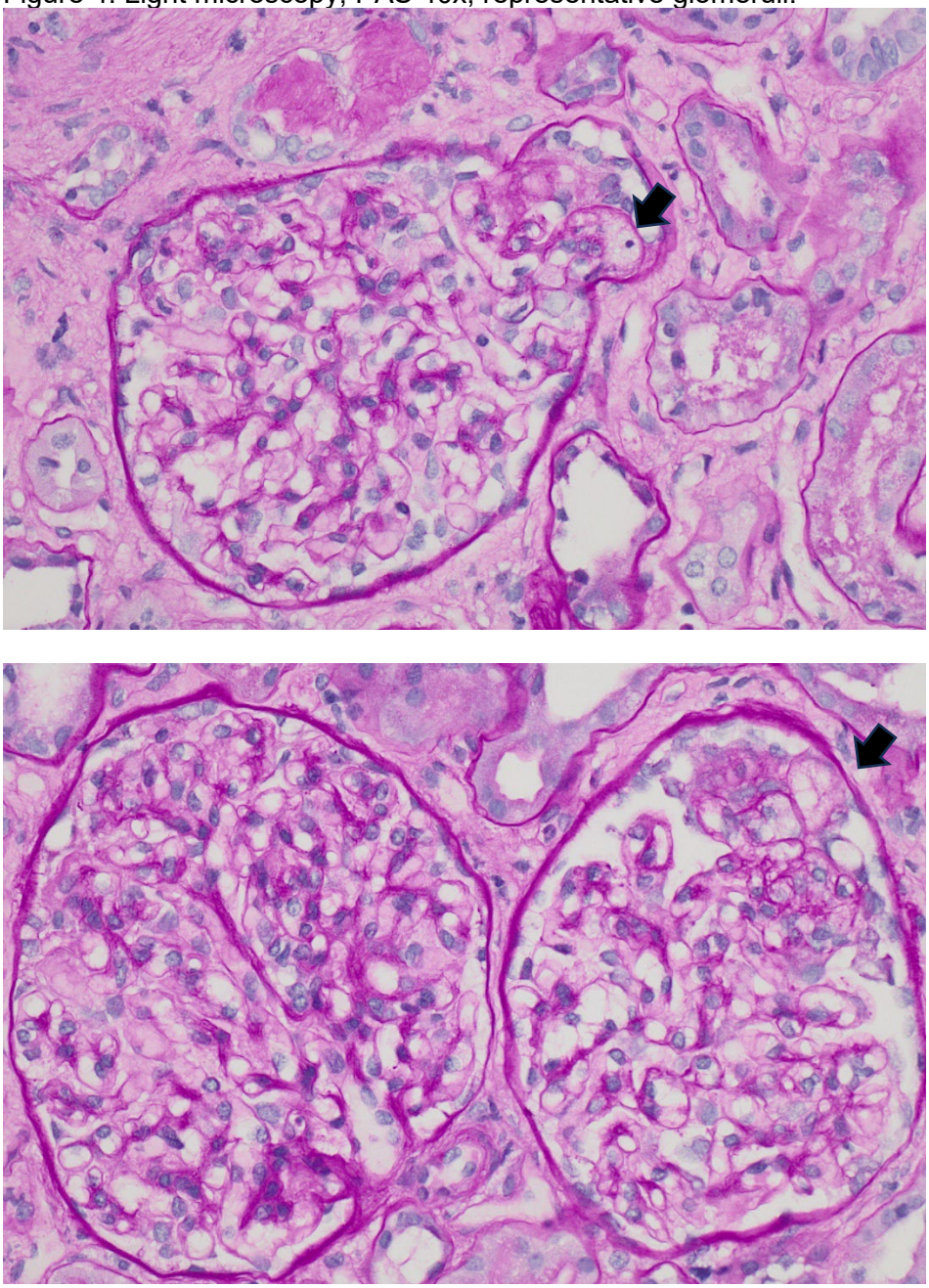

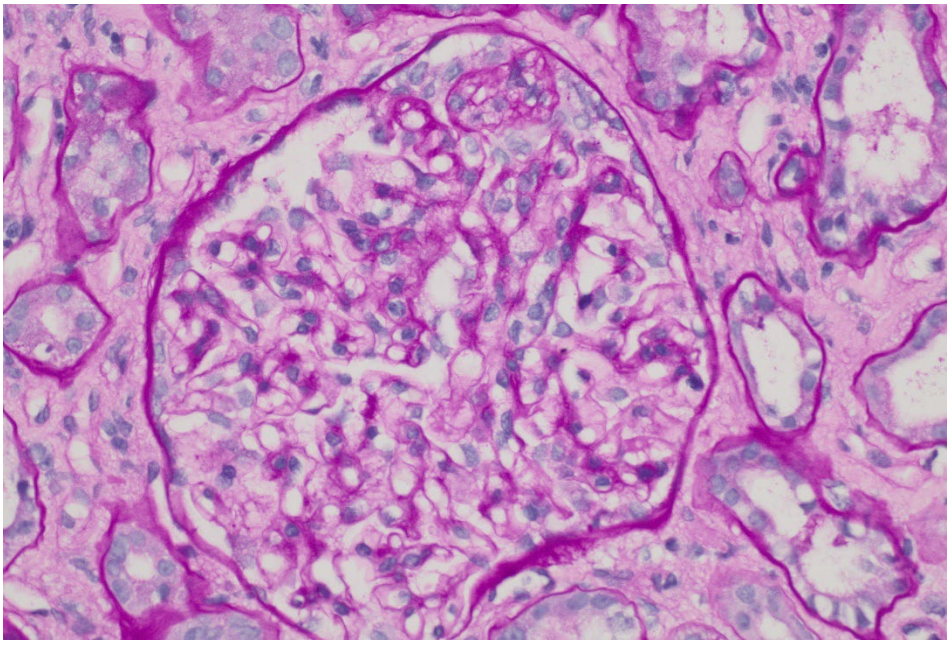

Figure 5. Light microscopy, Jones silver stain 40x, representative glomeruli:

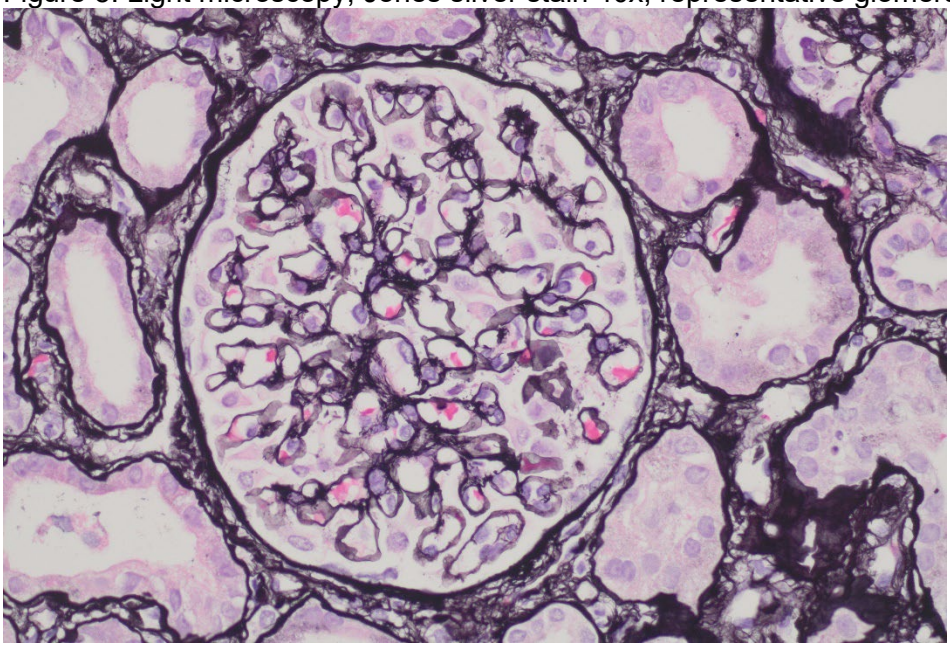

Figure 6. Immunofluorescence, IgG:

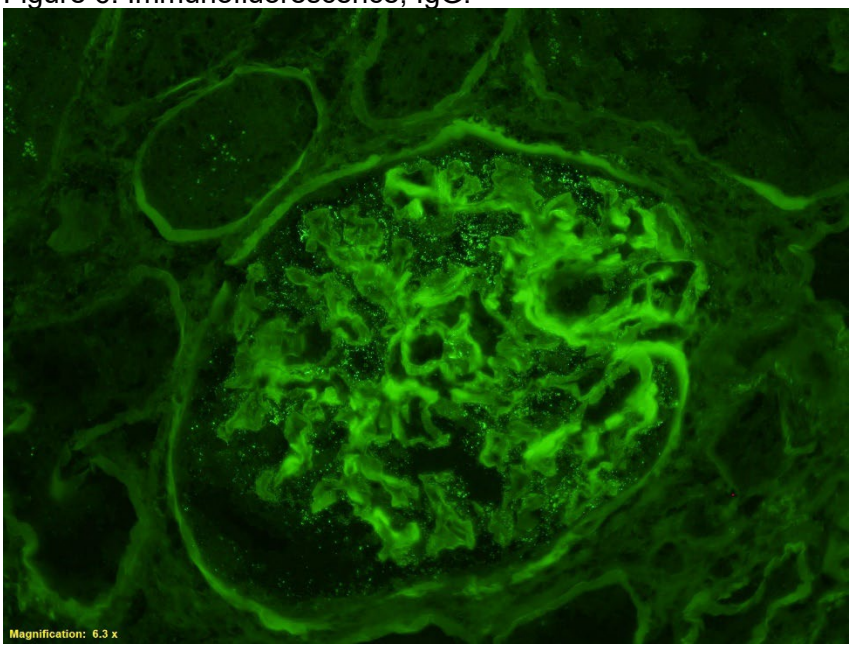

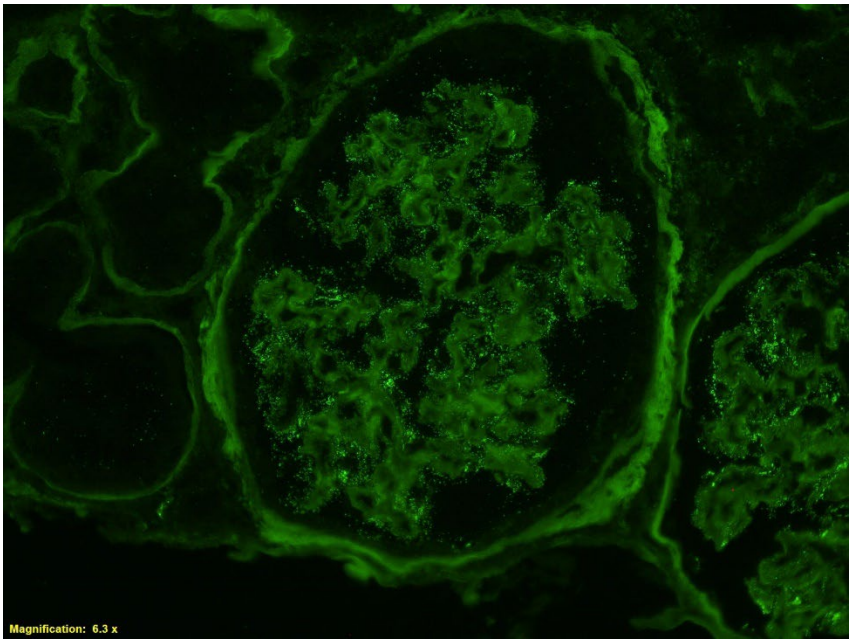

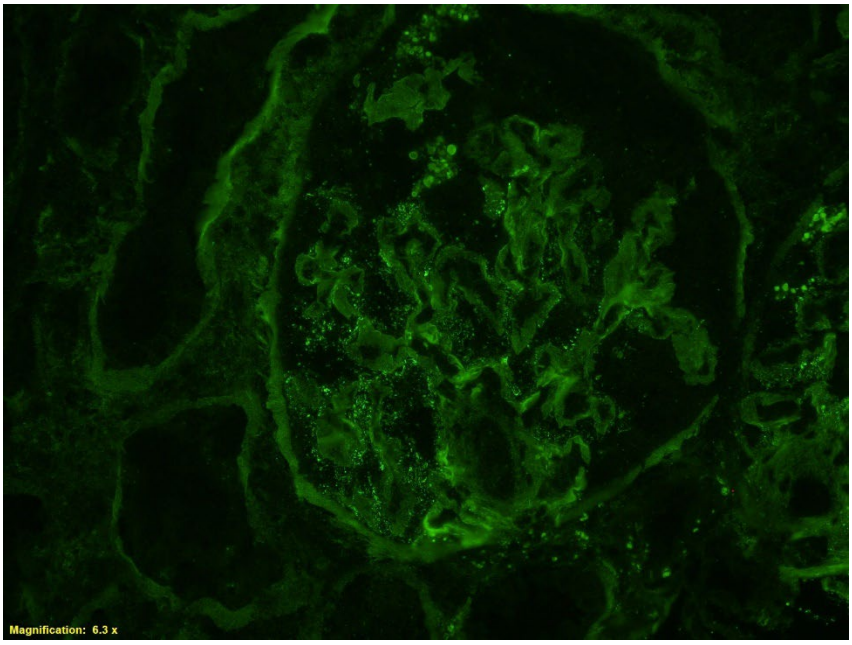

Figure 7. Immunofluorescence, IgG (green) + nephrin (red):

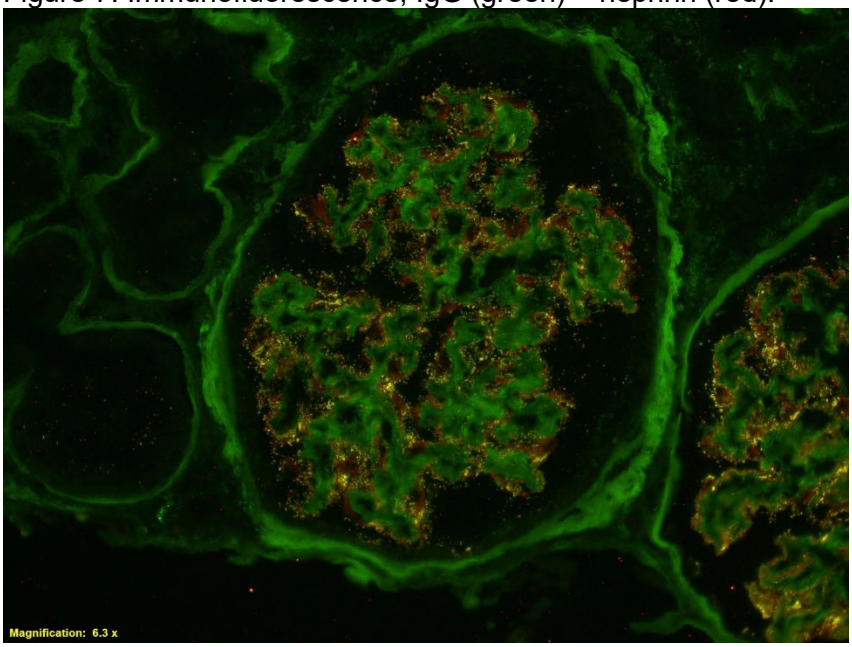

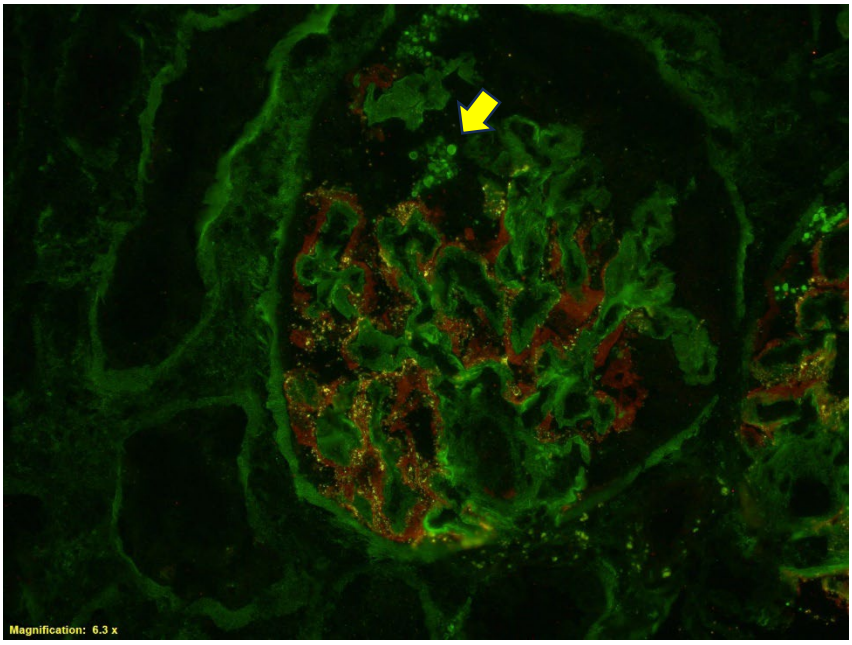

Figure 8. Electron microscopy, representative:

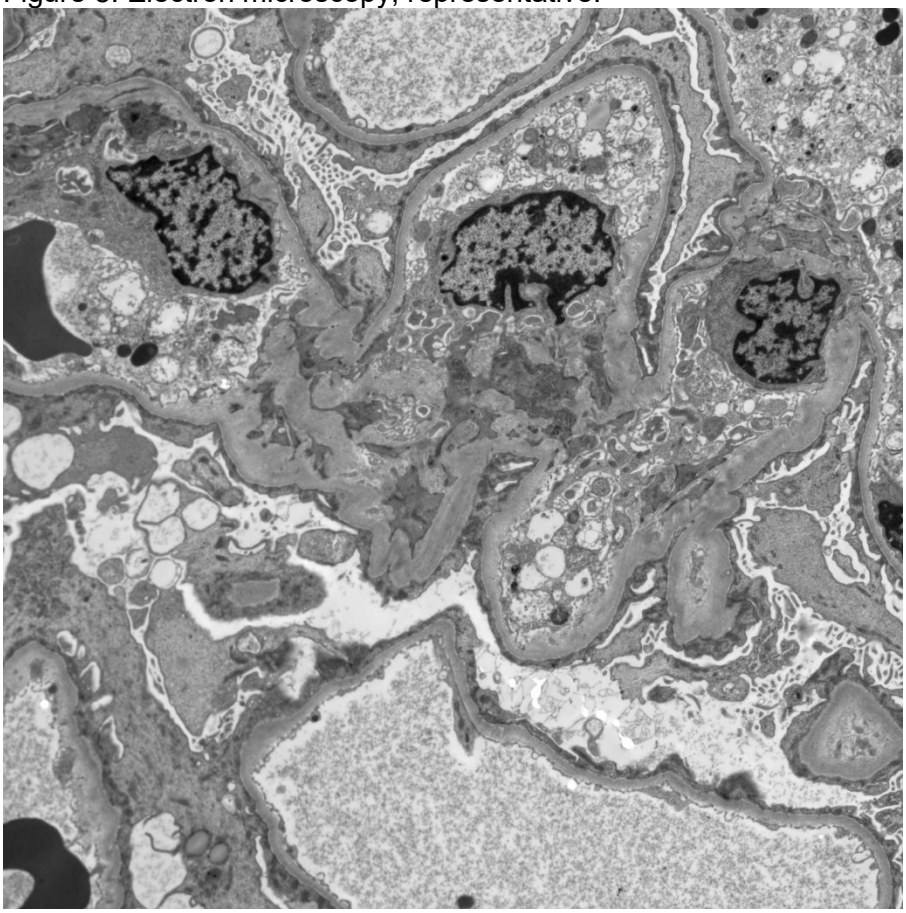

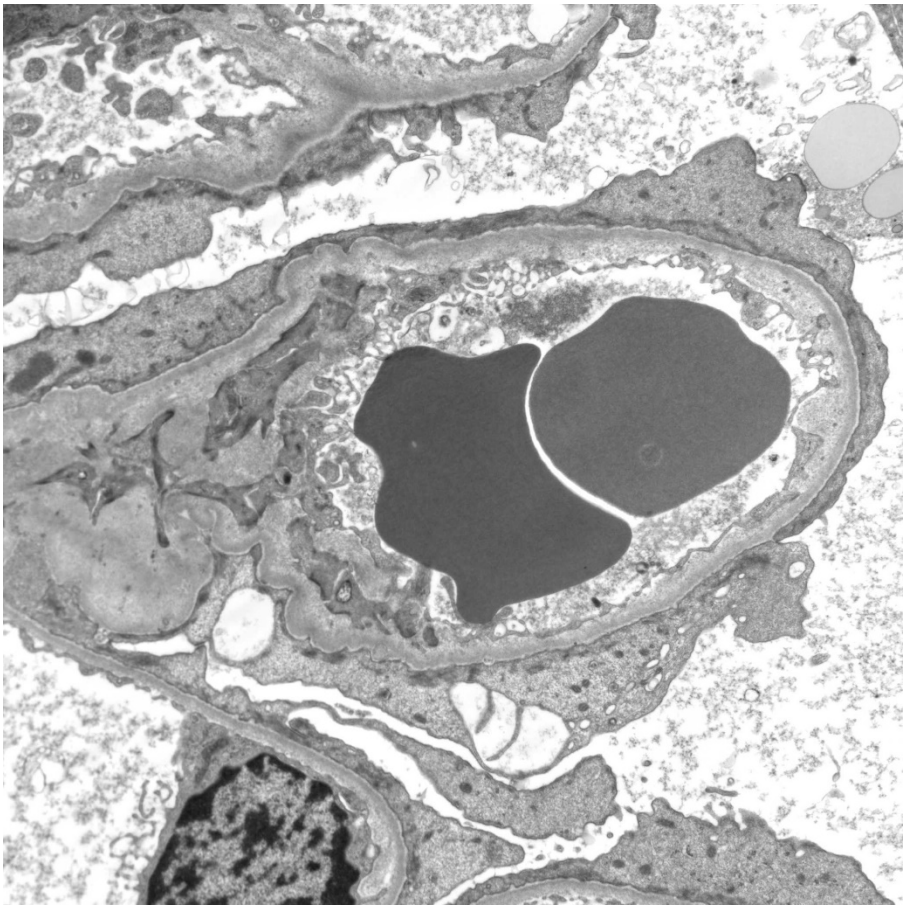

Pathologic Findings

Light Microscopy: The biopsy consists of renal cortex and medulla, with mild background tubular atrophy and interstitial fibrosis (Figure 1); there is no significant interstitial inflammation. Tubules reveal mild acute injury, and many tubular epithelial cells contain protein reabsorption granules (Figure 2). There are 57 total glomeruli (33 in the light microscopy sample), of which two are globally sclerosed, and 10 reveal tip lesions and early segmental sclerosis, with foam cells in the capillary loops (Figures 3–4; black arrow). The glomeruli are of normal size and cellularity. The capillary loops are of normal thickness and texture, without basement membrane spikes, holes/craters, or double contours (Figure 5). There is no endocapillary hypercellularity, segmental sclerosis, or crescentic injury. Arteries and arterioles show mild sclerosis.

Immunofluorescence: The sample contains 15 total glomeruli, five of which reveal suggestion of segmental sclerosis and evidence of podocyte cytoplasmic protein reabsorption granules. Fine granular staining (“dusting”) for IgG is noted over the podocytes (Figure 6), with similar staining for kappa and lambda light chains (not shown), and further staining with nephrin (red) and IgG (green) reveal colocalization (yellow) in the “dusting” (Figure 7). This colocalized staining is not seen in the larger epithelial cell protein reabsorption granules (Figure 7; yellow arrow) or in the tubular epithelial cell protein reabsorption granules (not shown). There is no significant granular staining along the capillary loops or in the mesangium, interstitium, or tubular basement membranes. There is no difference in reactivity for kappa and lambda light chains.

Electron Microscopy: Two glomeruli, one with early segmental sclerosis, are evaluated. There is global and diffuse foot process effacement (Figure 8), and the podocytes reveal extensive

microvillous degeneration. The segmentally sclerosed glomerulus reveals evidence of capillary loop foam cells. Electron-dense deposits are not seen along the glomerular capillary loops or in the mesangium. The basement membranes are attenuated (224 nm).

Diagnosis

- Diffuse podocytopathy with early FSGS/tip lesions, antinephrin-mediated
- Acute tubular injury
- Thin GBMs

Clinical Follow-Up

One week after biopsy, the patient is seen in clinic and, in conjunction with the findings on biopsy, is started on high-dose steroids (60 mg daily) in addition to aggressive diuresis. At that time, his urine protein/creatinine ratio is 13.6 g/g.

At follow-up three weeks later, his weight is down to 155 pounds (initial presentation at 230 pounds), and his edema has resolved. His urine protein-to-creatinine ratio is 4.5 g/g, although his serum albumin remains low (1.7 g/dL). His serum creatinine has also stabilized to baseline (1.1 mg/dL). Prednisone is decreased to 40 mg daily, with a plan to slowly taper over a few months, while concurrently initiating tacrolimus therapy (1 mg twice daily, with slow uptitration).

At follow-up four months later, he has weaned off steroids and is taking tacrolimus 3 mg twice daily. His urine protein-to-creatinine ratio is 955 mg/g, serum albumin 3.8 g/dL, and serum creatinine 1.13 mg/dL.

At follow-up three months later (nine months after biopsy), his urine protein-to-creatinine ratio is 1 g/g, serum albumin 4.4 g/dL, and serum creatinine 1.22 mg/dL. The last clinical note mentions that as he has only achieved partial remission on tacrolimus, the possibility of rituximab will be discussed (1 g at time zero and at 14 days, with a repeat dose in six months).

Questions for Case 4

1. What is the glomerular pattern of injury seen on the light microscopy samples?

A. Crescentic
B. Membranoproliferative
C. Mesangial hypercellularity
D. Membranous
E. Tip lesions/segmental glomerulosclerosis

The glomeruli on both H&E- and PAS-stained sections reveal the presence of glomerular foam cells, which can be seen in the setting of FSGS tip lesions (E). The glomeruli otherwise appear unremarkable. There is no cellularity in Bowman space, a.k.a. extracapillary hypercellularity or crescents (A), and there is no significant endocapillary hypercellularity (B). The mesangial regions do not reveal ≥4 nuclei (C). Jones silver stain demonstrates open capillary loops with uniform GBMs, which do not reveal the presence of spikes or holes/craters (D) or double contours (B).

2. How do you interpret the immunofluorescence findings from Figure 5?

A. Linear glomerular capillary wall staining for IgG
B. Fine granular capillary wall staining for IgG
C. Fine granular staining for IgG over the podocytes ("dusting")
D. Mesangial staining for IgG

Immunofluorescence microscopic examination of the glomeruli reveals a fine granular staining pattern by IgG (and kappa and lambda light chains, not shown). Importantly, this fine granular "dusting" pattern is seen in the urinary space (C) and not along the capillary walls (B), as would be seen in membranous nephropathy. The staining is not in the mesangium (D), as could be seen in systemic autoimmune- or infection-associated processes, and the pattern is granular and not linear (A), as can be seen in anti-GBM disease.

3. What is the pattern of injury seen on electron microscopy?

A. Subepithelial capillary deposits
B. Diffuse foot process effacement without associated capillary loop deposits
C. Subendothelial capillary loop deposits
D. Mesangial deposits and hypercellularity
E. Normal glomerular capillary loops

Electron microscopy images show capillary loops with diffuse foot process effacement, along with microvillous podocyte degeneration (B). There are no appreciable electron-dense deposits in the subepithelial (A), subendothelial (C), or mesangial (E) locations.

Discussion

Diffuse podocyte injury, encompassing both MCD and primary FSGS, is diagnosed by a morphologic finding of global foot process effacement on ultrastructural examination, with associated loss of slit diaphragms between adjacent foot processes, and by the clinical finding of overt nephrotic syndrome. By light microscopy examination, the findings vary based on the qualifier—MCD will show minimal glomerular alterations, whereas primary FSGS will show evidence of so-called tip lesions and/or more pronounced segmental glomerulosclerosis. Given these similar clinical presentations and histologic features, MCD and primary FSGS (and "idiopathic nephrotic syndrome", a diagnosis given to children with nephrotic syndrome who frequently are treated without kidney biopsy) are assumed to exist within a disease spectrum.

Recent studies have highlighted the presence of antinephrin antibodies in a proportion of MCD and primary FSGS cases. Further studies also suggest that the presence of pretransplant circulating antinephrin antibodies can predict post-transplant recurrent FSGS. These studies have found the presence of antinephrin antibodies in various proportions of both MCD and primary FSGS cases, found to be as high as 70% of untreated active MCD cases. Additionally, a proportion of children with steroid-resistant nephrotic syndrome have been found to have circulating antinephrin antibodies.

On immunofluorescence microscopy, the presence of this antibody can be seen by the presence of very fine granular "dusting"—punctate reactivity for IgG that is present in the urinary spaces and not along the GBMs (which is the typical immunofluorescence finding in membranous nephropathy, another cause of nephrotic syndrome). Further evaluation of this "dusting" reveals colocalization of IgG and nephrin. Nephrin is an important structural

component of the slit diaphragm complex that links adjacent podocyte foot processes and plays an important role in glomerular filtration.

This finding of antinephrin antibodies in diffuse podocytopathy further supports an autoimmune etiology, which could have clinical relevance in the treatment of patients with proteinuria. While corticosteroids remain the first-line therapy, concerns include high relapse rates and the side effect profile of corticosteroids. Calcineurin inhibitors are also used; with comparable efficacy and the benefit of reducing the risk of steroid-related complications, this class of medications comes with its own concern about long-term nephrotoxicity. Similar concerns exist for other second-line agents, including cyclophosphamide and mycophenolate. The finding of an autoimmune etiology could provide a further push in the use of rituximab, a monoclonal anti-CD20 antibody, to treat diffuse podocytopathy, regardless of the histopathologic appearance on biopsy. The early antinephrin studies included several patients who were treated with rituximab and achieved immunological and clinical remission through B cell depletion.

References

1. Watts AJB, Keller KH, Lerner G, et al. Discovery of autoantibodies targeting nephrin in minimal change disease supports a novel autoimmune etiology. *J Am Soc Nephrol*. 2022; 33:238-252.
2. Hengel FE, Dehde S, Lassé M, et al. Autoantibodies targeting nephrin in podocytopathies. *N Engl J Med*. 2024; 391:422-433.
3. Shirai Y, Miura K, Ishizuka K, et al. A multi-institutional study found a possible role of anti-nephrin antibodies in post-transplant focal segmental glomerulosclerosis recurrence. *Kidney Int*. 2024; 105:608-617.
4. Batal I, Watts AJB, Gibier J, et al. Pre-transplant anti-nephrin antibodies are specific predictors of recurrent diffuse podocytopathy in the kidney allograft. *Kidney Int*. 2024; 106:749-752.
5. Raglianti V, Angelotti ML, Cirillo L, et al. Anti-slit diaphragm antibodies on kidney biopsy identify pediatric patients with steroid-resistant nephrotic syndrome responsive to second-line immunosuppressants. *Kidney Int*. 2024; 106:1124-1134.
6. Zhong A, Yu Y, Cao T, et al. Emerging role of Rituximab in adult minimal change disease: a narrative review of clinical evidence, biomarkers and future perspectives. *BMC Nephrol*. 2025; 26:152. DOI: 10.1186/s12882-025-04086-3.
7. Ichikawa Y, Sakakibara N, Aoyama S, et al. Co-localization of IgG with nephrin in immune-mediated idiopathic nephrotic syndrome. *Clin Exp Nephrol*. 2025. DOI: 10.1007/s10157-025-02741-5.